

# **Design, Analysis and Remote Monitoring of a Solar Powered Orphan Oil Well Pumping System in Nigeria**

Written by

©Chidolue Onyinyechukwu

A Thesis Submitted to the School of Graduate Studies in partial fulfillment of  
the requirements for the degree of

Master of Engineering

Faculty of Engineering and Applied Science  
Memorial University of Newfoundland

October 2023

St. John's

Newfoundland and Labrador

Canada

## **Abstract**

This thesis explores the issue of orphaned wells, which are abandoned oil and gas wells left uncapped, leading to the release of greenhouse gases, including methane and hydrogen sulphide gas  $H_2S$ , which is lethal to humans into the atmosphere. These wells contribute significantly to global warming, as methane is a potent greenhouse gas with a high heat-trapping capability, unfortunately due to it cost an average of 100,000CAD per well for oil well plugging, most oil industry abandon these wells. The research identifies cost-effective strategies to mitigate the impact of abandoned wells using renewable technology, specifically focusing on a comprehensive system sizing approach for Olobiri oil well 17. To address the problem, the study recommends the use of solar-powered pumps to remove the remnants of oil from the wells. PVsyst software is employed to determine the appropriate pump size if the system ran continuously or solar peak hours of the location. The results demonstrate that a 5-hour running time yields higher system efficiency compared to continuous running time. Based on HOMERpro optimization result, a 50kW PV unit and 54.9kW batteries are recommended for the system setup, resulting in improved efficiency and cost-effective option during the 5-hour operation with an overall efficiency of 11.4% and pump efficiency was 37.9% compared to a continuous flow system efficiency of 5%, and the pump efficiency of 11%. For monitoring and data logging purposes, the addition of PLX DAQ aids in real-time monitoring system for the design characteristics such as PV voltage and current, inverter AC output, oil level and temperature. This low-cost data logging system allows for easy maintenance and provides valuable data for further analysis since the PLX DAQ is a Microsoft Excel's add-on. Also, due to the site location and the specification describing the location, Lora Technology is implemented for real time monitoring, which is independent on the internet network. In conclusion, this research highlights the importance of addressing orphaned wells'

environmental impact and proposes a viable solution for capping using renewable technology, particularly solar-powered pumps, to mitigate greenhouse gas emissions and the potential hazards posed by abandoned wells.

## **Acknowledgement**

First and foremost, I extend my heartfelt gratitude to the Lord Almighty, as well as the Chidolue's and Edeh's family, for their unwavering support throughout my academic journey. I am immensely thankful to my late sister and father, who have been a source of inspiration as pioneers. I want to express my sincerest appreciation to my supervisor, Dr. Mohammad Tariq Iqbal, whose mentorship has been invaluable. Our journey together, starting from my role as a Teaching Assistant to becoming his graduate student, has been a truly enriching experience. His belief in my abilities has led to various opportunities and accolades during my graduate studies, for which I am truly grateful. I also wish to acknowledge the generous support provided by Glofshan Limited, which allowed me to fully dedicate myself to my research endeavors. Their financial assistance played a crucial role in my academic success. Lastly, I extend my thanks to Memorial University of Newfoundland for providing a nurturing institution that allowed me to thrive. Additionally, I want to express my gratitude to my dear friends, Maryrose, Chisom, and Uche, who have been my pillars of strength and support during the challenging times of my journey. Their presence has been nothing short of a therapeutic system that uplifted me along the way.

## Table of Contents

<b>Abstract</b> .....	ii
<b>Acknowledgement</b> .....	iv
<b>Table of Contents</b> .....	v
<b>List of Table</b> .....	viii
<b>List of Figures</b> .....	ix
<b>List of Abbreviations</b> .....	xii
<b>Chapter 1 Introduction</b> .....	1
1.1 Background.....	1
1.1.1 Orphaned Oil Well and its Effect to the Environment .....	2
1.1.2 Abandoned Oil in Nigeria .....	6
1.1.3 Oil and Gas Sector in Nigeria .....	7
1.1.4 Growing Investments in Oil Infrastructure .....	7
1.1.5 Abandoned Site Characteristics – Oloibiri oil field .....	8
1.1.6 The Oil Well Development .....	9
1.1.7 The Exploitation and Effects of the Abandoned Oil Fields in Oloibiri Community 12	
1.1.8 Solar energy in Nigeria and daily consumption .....	14
1.2 Problem Statement.....	16
1.3 Research Objectives .....	17
1.4 Thesis Organization.....	18
1.5 Bibliography .....	19
<b>Chapter 2 Design and Performance Analysis of an Oil Pump Powered by Solar for a Remote site in Nigeria</b> .....	23
2.1 Introduction .....	24
2.1.1 Recent Application of Solar Powered Pump in Oil Drilling .....	27

2.1.2	Upstream: Renewable Integration in Oil and Gas Production .....	30
2.1.3	Electric pumps in the oil and gas production .....	31
2.2	Site Characteristics – Oloibiri Oil Well 17 Field .....	32
2.3	System Design Calculation.....	33
2.3.1	Site Description .....	33
2.3.2	Solar Irradiance of the Site.....	33
2.3.3	Pump Sizing .....	34
2.4	Solar Pump Design by Pvsyst.....	36
2.4.1	Pump Sizing for a Running Time of 5 hours/day.....	36
2.4.2	Pump Sizing for continuous running time (non-stop).....	37
2.5	Pv Sizing by Homerpro Software .....	38
2.5.1	PV Panel and Battery Performance .....	42
2.6	System Performance .....	43
2.7	Conclusion.....	46
2.8	Bibliography .....	47
<b>Chapter 3 System Monitoring and Data logging using PLX-DAQ for Solar-Powered Oil Well</b>		
		<b>49</b>
3.1	Introduction .....	50
3.2	Literature Review .....	51
3.3	Methodology.....	52
3.4	P.L.X. - D.A.Q. and Syntax.....	53
3.4.1	Real-time instrumentation Circuit diagram and material .....	55
3.5	Results from Plx Daq.....	61
3.6	Conclusion.....	64
3.7	Bibliography .....	65

<b>Chapter 4 Real-Time Monitoring and Data Acquisition Using LoRa for a Remote Solar Powered Oil Well.....</b>	<b>67</b>
4.1 Introduction .....	68
4.1.1 Lora Sender .....	70
4.1.2 Lora Receiver .....	71
4.2 Wireless Communications .....	72
4.3 Advancement of Lora Technology .....	73
4.4 Methodology.....	75
4.4.1 Instrumentation Circuit Design and Calibration .....	76
4.4.2 LoRa code and syntax explanation for the system instrumentation.....	80
4.5 Results .....	81
4.6 Conclusion .....	85
4.7 Bibliography .....	86
<b>Chapter 5 Conclusion and Future Work.....</b>	<b>89</b>
5.1 Conclusion .....	89
5.2 Future Work.....	92
APPENDICES.....	95

**List of Table**

Table 3.1:TMP36 Specification ..... 59

**List of Figures**

Figure 1:1: Current Oil well State ..... 11

Figure 1:2: Oloibiri Oil well 1 currently used as a historical figure. .... 12

Figure 1:3: The current state of the oil well spillage and effect in the community. .... 14

Figure 1:4: The geographical solar irradiance range in Nigeria ..... 16

Figure 2:1: Solar Global Horizontal Irradiance for Oloibiri, Nigeria (HOMER) ..... 34

Figure 2:2: Input parameter for the system in PVsyst..... 36

Figure 2:3: PVsyst system sizing Suggestion ..... 37

Figure 2:4: PVsyst system sizing Suggestion ..... 37

Figure 2:5: Condition a Load Picture ..... 38

Figure 2:6: System Sizing Architecture ..... 39

Figure 2:7: Simulation result details ..... 40

Figure 2:8: System Sizing Architecture ..... 40

Figure 2:9: Condition B Load profile..... 41

Figure 2:10: Simulation result details ..... 41

Figure 2:11: Renewable Penetration details..... 42

Figure 2:12: Battery performance details..... 43

Figure 2:13: Battery performance details for 24 hours running time..... 43

Figure 2:14: Pre-sizing parameter, simulation parameters and results ..... 44

Figure 2:15: Pre-sizing parameter, simulation parameters and results ..... 44

Figure 2:16: Pre-sizing parameter, simulation parameters and results. .... 45

Figure 2:17: Pre-sizing parameter, simulation parameters and results. .... 45

Figure 2:18: Detailed System Design Diagram..... 46

Figure 3:1: Instrumentation Block Diagram ..... 53

Figure 3:2: PLX DAQ User interface .....	54
Figure 3:3: Circuit Diagram Schematic .....	55
Figure 3:4: Voltage Sensor image .....	56
Figure 3:5: Voltage divider embedded in the voltage sensor IC .....	57
Figure 3:6: ACS712 Model and Output Sensitivity .....	58
Figure 3:7: Current Sensor and the internal datasheet .....	58
Figure 3:8: TMP36, Temperature Sensor.....	59
Figure 3:9: Flowchart for the System Monitoring of PLX-DAQ.....	60
Figure 3:10: Data readings in Excel spreadsheet. ....	62
Figure 3:11: Overall data plot in Excel. ....	62
Figure 3:12: Oil level float switch status .....	63
Figure 3:13: Voltage, Current and Power data from a lab test setup .....	63
Figure 3:14: Temperature Data Chart .....	64
Figure 4:1: LoRa Sender Node FlowChart .....	71
Figure 4:2: Lora Receiver Node Flowchart.....	72
Figure 4:3: Instrumentation Block Diagram of the Entire Monitoring System .....	75
Figure 4:4: Temperature Sensor Circuit Connection. ....	77
Figure 4:5: Voltage Sensor Connecting Circuit .....	78
Figure 4:6: Voltage Divider rule embedded in the IC.....	78
Figure 4:7: ACS712 and Model Sensitivity .....	79
Figure 4:8: Current Sensor Connecting Circuit.....	79
Figure 4:9: Implemented Circuit with Sender Node .....	82
Figure 4:10: Receiver Node .....	83
Figure 4:11: Data Transmitted wirelessly to PuTTY .....	84

Figure 4:12: Data indicating that the Oil Level is high..... 85

## List of Abbreviations

AC	Alternating current
ADC	Analog-to-Digital converter
AECs	Alternative energy credits
AEPS	Alternative Energy Portfolio Standard
AO	Abandoned Oil and Gas
DAQ	Data acquisition
EIA	Energy Information Administration
ESP	Electric submersible pump
IoT	Internet of Things
LoRaWAN	Long Range Wide Area Network
LPWAN	Low Power Wide Area Networks
MPPT	Maximum Power Point Tracking
NNPC	Nigerian National Petroleum Corporation
PLX-DAQ	Parallax Data Acquisition
PV	Photovoltaic
RE	Renewable Energy
SPDC	Shell Petroleum Development Company of Nigeria Limited

# Chapter 1

## INTRODUCTION

### 1.1 Background

Renewable Energy (RE) technology harnesses naturally replenishable energy sources, such as solar, wind, hydro, geothermal, and biomass, and converts them into usable energy forms. Given the growing global population, the imperative to address global warming, and its impact on the ecosystem, it becomes essential to limit the consumption of fossil fuels, which currently serve as the primary energy source. Embracing renewable energy sources offers a sustainable approach to protecting the environment and mitigating the greenhouse effect associated with fossil fuel usage. Furthermore, predictions in [1] suggest that fossil fuel supplies will become constrained soon, potentially leading to depletion as the population continues to rise. Given the significance of climate change as a pressing global concern, renewable energy sources play a vital role in providing an environmentally friendly energy alternative that contributes significantly to climate change mitigation. According to a 2008 global energy evaluation, renewable energy sources accounted for approximately 12.9% of the total energy supply of 492 EJ (exajoules). Notably, biomass made the largest contribution at 10.2%, with approximately 60% of biomass fuel utilized for heating and cooking purposes. Hydropower constituted 2.3% of the total, while solar and other sources combined contributed about 0.4%.

From the global electricity supply data [2], renewable energy accounted for 19% of the total, with hydropower being the most prominent at 16%, and other renewable sources making up 3%. For transportation energy supply, biofuels contributed 2%, biomass 8%, and traditional fuels represented 17%. When considering heating on a global scale, solar and geothermal energy combined to contribute about 27%. Although renewable energy consumption remains

relatively low and may not yet meet the rapidly increasing demand for energy, there has been a noticeable increase in the deployment of renewable energy technologies in recent years.

Enhancing the productivity of oil drilling operations within the oil and gas sector can be achieved by integrating renewable energy sources to power the pumping units. Considering the escalating demand for crude oil coupled with its finite supply, adopting this technology can effectively reduce the production costs associated with fossil fuel-driven pumps in the drilling system [3]. It becomes essential to develop technologies that can lower drilling expenses, offer sustainable power solutions, minimize maintenance costs, and mitigate oil spillage caused by mechanical pumping. Such oil drilling spills have significant environmental impacts, affecting marine life and seafloor ecosystems [4]. The toxic oil spillage can disrupt the food chain, highlighting the importance of transporting oil from reserves to storage without spillage and reducing drilling costs [4]. This research endeavors to concentrate on developing a renewable technology utilizing photovoltaic systems, enabling the monitoring and power supply for oil pumps. The monitoring units will include mechanisms of LoRa Technology and Internet of Things to monitor oil levels in the tank, notifying when oil reaches a specified level, thus reducing the likelihood of spillage during the drilling process. Additionally, the Maximum Power Point Tracking (MPPT) feature will optimize the operation of the photovoltaic system, ensuring it functions at its maximum efficiency point.

#### 1.1.1 Orphaned Oil Well and its Effect to the Environment

Over time, as wells ran dry and their operators face financial difficulties, many wells are abandoned without proper capping. Consequently, their deteriorating pipes are left behind in remote areas that later developed into towns, cities, and suburbs. Some operators neglect to seal the wells, while others used makeshift methods with materials like scrap lumber or construction debris. These abandoned and inadequately plugged wells are commonly known as orphaned

wells. If not drilled correctly, these wells can emit greenhouse gases into the atmosphere for extended periods. It is now widely recognized that orphaned wells contribute to the issue of global warming.

In the United States, there is an extensive number of abandoned oil and gas wells, totaling over 3.2 million. These wells were left behind for various reasons, becoming obsolete over time. Additionally, there is another category of wells known as "stripper wells," responsible for extracting the last reserves from depleting oilfields. Stripper wells are characterized by producing fewer than 15 barrels of oil per day, and it's estimated that the United States has around 380,000 such wells, some of which are in poor condition and causing environmental harm. Both types of wells, abandoned and stripper wells, fall under the regulation of state oil and gas regulatory organizations, such as Texas's Railroad Commission. The environmental hazards resulting from spills can have far-reaching consequences, impacting not only local wildlife but also agriculture and human health. Abandoned gas wells continue to pose a significant threat by polluting freshwater aquifers, rivers, lakes, and the air we breathe across the United States.

Methane, a potent greenhouse gas, is approximately 100 times more effective at trapping heat in the atmosphere compared to CO<sub>2</sub>. In the United States alone, abandoned wells are believed to have released 281 kilotons of methane into the atmosphere, equivalent to the emissions of over 400 large oceangoing LNG transport ships annually [5].

Abandoned and marginal oil wells can also release hazardous substances like hydrogen sulphide gas ( $H_2S$ ), which is lethal to humans. The "rotten egg" smell of  $H_2S$  is a familiar issue in small communities situated close to oil and gas wells, though it is usually present in low quantities not sufficient to be fatal. For example, residents of Luling, Texas, have experienced

this distinct odor coming from ancient oil wells. Additionally, some wells contribute to salt-water leaks. As oil wells age, they often produce substantial amounts of salt water, which is usually separated from the oil at the surface using specific tanks. If these separation systems are not adequately maintained, small amounts of oil and salt water can escape into the environment, causing harm to marine life in rivers and ponds and leading to soil degradation due to excessive salt accumulation [6].

The expenses associated with methane emissions from Abandoned Oil and Gas (AOG) wells rely on the emission rate, which can exhibit significant variations across different scales [7,8]. Methane emissions from AOG wells follow extreme probability distributions, with the most substantial 16% of leaks ( $> 0.09$  tonne yr<sup>-1</sup> well<sup>-1</sup> or  $> 104$  mg h<sup>-1</sup> well<sup>-1</sup>) accounting for 98% of the total leakage volume [7, 9]. It is imperative to identify cost-effective strategies to mitigate the impact of AOG wells since many of these wells are under the responsibility of government agencies with limited financial resources [10]. For instance, in Pennsylvania, the PA DEP (Pennsylvania Department of Environmental Protection) is tasked with plugging tens to hundreds of thousands of AOG wells; however, only 1679 wells were plugged by the PA DEP between 2004 and 2013. Additionally, there is a growing concern, as observed in Canada, where abandoned wells from bankrupt companies raise environmental issues due to the lack of sufficient incentives for cleanup [11]. The cost of plugging AOG wells can range from approximately \$10,000 to around \$1,000,000 per well, necessitating exploration into alternative or supplementary mitigation strategies and their associated costs. Strategies that have been successfully employed to reduce methane emissions in active oil and gas systems and coal mines can also be applied to AOG wells. These strategies fall into three broad categories: plugging, flaring, and recovery/utilization of emitted gases [12, 13]. Flaring involves burning methane, converting it into CO<sub>2</sub> and water, while utilization options include using methane

directly as a fuel, connecting it to natural gas pipelines for off-site use, or re-injecting it for enhanced oil recovery [13,14] Both flaring and utilization can be applied to both plugged and unplugged AOG wells. All the methods mentioned are either economically intensive or require a lot of technology and labour for extraction. These researches present a cheap labour and cost of implementation that extracts the remains from depleting oilfields.

### ***Energy Saving from Captured Methane***

The gases captured from AOG wells present a potential alternative energy resource within the framework of Pennsylvania's Alternative Energy Portfolio Standard (AEPS) program. This program, designed to promote renewable energy adoption, includes various renewable and non-renewable sources. The alternative energy sources in AEPS are divided into two categories: Tier I and Tier II. Tier I primarily encompasses renewable sources such as solar, wind, and biomass, but also includes coal mine methane, which bears similarities to the gases emitted by AOG wells. Tier II, on the other hand, includes large-scale hydropower, demand-side management, and municipal solid waste. To determine the eligibility of gas emitted from AOG wells as an alternative energy resource, it relies on the interpretation of current regulations and may necessitate explicit modifications to encompass AOG wells [15].

The AEPS program creates a demand for alternative energy by imposing specific requirements on electric distribution companies and electric generation suppliers, mandating that a certain percentage of total energy sold must be sourced from alternative energy. Additionally, the AEPS offers monetary incentives through the allocation of alternative energy credits (AECs), earned for each megawatt hour (MWh) of alternative energy produced. To convert Gases captured  $S_{a,MWh}$  to savings,  $s_a$  (price per tonne CH<sub>4</sub> emissions avoided), we determine the equivalent amount of natural gas necessary to generate 1 MWh of electricity.

Therefore,

$$S_a = \frac{S_{a,MWh} * h}{rdC} \quad (1)$$

Where h is the fuel heat content (BTU/ $ft^3$ ), r is the heat rate (BTU/kWh), d is the density (tonne/ $m^3$ ), and C is the conversion factor of 28.31682  $m^3$  /Mcf.

### 1.1.2 Abandoned Oil in Nigeria

The House of Representatives has directed the Committees on Petroleum Resources (Upstream) and Environment to investigate the causes of oil spills at OML 18, OML 29, and OML 63, as well as the issue of abandoned wells in the Niger Delta region. The source of the oil spill at OML 18 is the dormant and remote Cawthorne Channel Well 15. Eroton Exploration and Production Limited, in a joint venture with the Nigerian National Petroleum Corporation (NNPC) Limited after Shell Petroleum Development Company of Nigeria Limited (SPDC) divested its interest in the bloc, operates the significant oil bloc south of Port Harcourt, Rivers State. In OML 29, the Santa Barbara Oil Company reported an oil leak from their inactive and remote Santa Barbara oil well head 1 in Nembe Local Government Area (LGA) of Bayelsa State on November 5, 2021. The leak, lasting for 32 days, impacted the Santa Barbara River and its tributaries, affecting farming, fishing, and drinking water in three kingdoms of Bayelsa State. The cause of this oil leak on OML 29 remains unknown even after six months [18].

The ongoing oil leak issue at OML 18 has not been investigated yet, two weeks after the incident, unlike OML 29. Similarly, the root cause analysis for the month-long oil leak at OML 63 in Lasukugbena, Bayelsa State, has not been formally established. It is worth noting that there are up to 800,000 barrels of remaining crude oil resources in Nigeria's various oil fields, which are currently producing less crude oil than before, but still hold significant economic value [18].

### 1.1.3 Oil and Gas Sector in Nigeria

Nigeria stands as one of Africa's largest countries in terms of its considerable proven reserves of oil and gas. As of 2020, the country's proven crude oil reserves were measured at 86.9 million tonnes, while its natural gas reserves were approximately 49.4 billion cubic meters (bcm). Notably, Nigeria produces low-sulfur crude oil, which is highly sought after globally due to the increasing demand for products with reduced sulfur content processed by refineries worldwide. The expected surge in demand for Nigerian low-sulfur crude oil is anticipated over the study period [19, 20].

The global shipping industry has already adapted to the International Maritime Organization's (IMO) new bunker sulfur cap of 0.5%, which came into effect on January 1, 2020. As a result, the Nigerian upstream industry is poised to experience substantial investment because of the IMO regulations and the growing need for petroleum with low sulfur content. Recent developments, such as the commencement of oil production from Nigeria's Anyala West field in the shallow offshore blocks OML 83 and 85 by FIRST E&P and the state-owned Nigerian National Petroleum Corporation in November 2020 are also expected to contribute to market growth. Given these factors, the upstream sector is predicted to witness significant growth throughout the projection period [19, 20]

### 1.1.4 Growing Investments in Oil Infrastructure

Nigeria holds a prominent position as one of Africa's largest and oldest oil producers, with its oil and gas industry playing a vital role in the national economy. More than 90% of Nigeria's exports and approximately 80% of the federal government's income come from this industry. The country boasts the ninth-largest oil reserves globally, estimated at around 193.3 trillion cubic feet (Tcf). However, there have been no recent developments in new gas projects. As of

2020, Nigeria possessed the most substantial oil and gas reserves in Africa, with approximately 37 million barrels of crude oil (36,910 million barrels) and 5.5 trillion cubic meters of gas. Looking ahead, the country aims to position itself as an African export hub, not only catering to regional countries but also targeting other Asian nations like India and China, where the demand for gas is projected to increase in the coming years [19].

Moreover, there is a substantial domestic demand for oil in the country, primarily driven by the power industry. The existing fossil-fuel power facilities often face underutilization due to inconsistent supplies. Finding solutions to enhance crude oil production is essential, and integrating renewable energy into the production process could help alleviate the issue. Because of the mentioned challenges, increased investments in natural gas infrastructure are expected to drive growth in Nigeria's oil and gas sector in the projected period. Incorporating renewable energy into oil drilling operations should also aid in reducing the economic costs associated with production.

#### 1.1.5 Abandoned Site Characteristics – Oloibiri oil field

The Oloibiri Oilfield is located around 45 miles (72 km) east of Port Harcourt in the Niger Delta, specifically in Oloibiri, Ogbia Local Government Area (LGA), Bayelsa State, Nigeria. It falls within Oil Mining Lease 29 (OML 29) and covers an area of approximately 13.75 square kilometers (5.31 square miles). The name of the oilfield is derived from the nearby small stream village of Oloibiri where it is situated. Currently, the field is managed by the Shell Petroleum Development Company of Nigeria Limited (SPDC). Notably, this oilfield marked Nigeria's first successful commercial oil discovery, bringing an end to 50 years of unsuccessful oil exploration efforts by various foreign oil companies and propelling the nation into the global spotlight as a Petro-State [21].

On August 3, 1955, the exploration well known as Oloibiri 1 was drilled vertically to a depth of 108 feet (3660m). Upon testing, it was identified as a commercial discovery, producing oil at a rate of approximately 5,000 barrels (790 m<sup>3</sup>) per day, alongside some gas. The field commenced oil production between late 1957 and early 1958, with an initial output of 4,928 barrels of oil per day (783.5 m<sup>3</sup>/d). During the first year, the average daily production was 5,100 barrels of oil. As additional wells were completed and put into operation, the output increased, reaching its peak in 1964. A total of eleven productive wells were employed for reservoir drainage. The oil extracted from the field is characterized as heavy, sour, with an API rating of 20.6 [22, 23, and 24]. During that period, due to the lack of gas processing and utilization facilities in the country, the gas co-produced with the oil was flared as it was considered unnecessary. To access export facilities, Royal Dutch Shell constructed the first crude oil pipeline in Nigeria, connecting the Oloibiri field to Port Harcourt on the Bonny River. The Oloibiri oil field in Nigeria commenced its first crude oil exports in February 1958, initially producing at a rate of 5,100 barrels per day (810 m<sup>3</sup>/d). To facilitate oil transportation from the field, Shell constructed the nation's inaugural pipeline. Over its operational span of 20 years, the Oloibiri oilfield yielded more than 20 million barrels (3,200,000m<sup>3</sup>) of oil. However, in 1978, oil production ceased, and the field was officially closed down the following year [25, 26]. Despite the presence of approximately 2,126,000,000 barrels (3380000m<sup>3</sup>) of hydrocarbons remaining in the site, no enhanced recovery methods were employed, leading to the abandonment of the Oloibiri oilfield.

#### 1.1.6 The Oil Well Development

In the process of developing the field, four development wells were drilled in 1958 between June 17 and November 27, following the successful completion of the field's appraisal. These

six effective appraisal wells, along with the four development wells, were converted into operational oil production wells.

On June 5th, 1956, the discovery well, Oloibiri-1, underwent renovation and transitioned into an active oil well. Marking Nigeria's first commercially viable oil well, Oloibiri-1 created a historic milestone. With this, the total number of finished production wells in the field reached eleven. To assess the extension of the reservoir to different areas, a total of 11 appraisal wells were drilled vertically between June 26, 1956, and October 28, 1958 [21, 22]. The initial appraisal well, Oloibiri-2, was drilled to a depth of 2932 meters on June 26, 1956, and it discovered oil in the Agbada Formation. These six appraisal wells were successful and yielded oil pay. However, after nine years of production, the Oloibiri-17 appraisal well was spudded on June 9th, 1967, and drilled to a measured depth of 12520 feet; unfortunately, it did not yield promising results and has been plugged. During this time, the field was nearly depleted, and it was considered a stripper well, producing below 15 barrels per day

The field's production has experienced a decline from its peak level. Another evaluation well, Oloibiri-18, was spudded on April 21 and drilled to a vertical depth of 9616 feet (2931 m). Unfortunately, the results were impressive. The primary purpose of Oloibiri-18 was to assess a new section of the reservoir and improve drainage, but due to its dry condition and signs of deterioration, the well was plugged and left unattended [21, 22].



Figure 1:1: Current Oil well State



Figure 1:2: Oloibiri Oil well 1 currently used as a historical figure.

### 1.1.7 The Exploitation and Effects of the Abandoned Oil Fields in Oloibiri Community

According to a source cited in Sunday Vanguard [25], the impact of oil exploration and exploitation is evident across various aspects of life. The marine ecosystem has suffered irreparable damage, leading to the extinction of marine life. Indigenous occupational industries have been severely affected, and erosion has become widespread. Furthermore, pollution of essential resources, such as water used by ordinary people for drinking and fishing, has become

a prevalent issue. The oil company involved in these activities has been accused of demonstrating insensitivity towards the situation. Despite providing poorly structured amenities like electricity, water, high-powered marine transport vehicles, and health facilities at the drilling sites at the time of its operation, which . There is a significant disparity in living standards presently in the community and the abandoned oil well facilities. According to the natives of Otuabagi community, who are recognized as the original property owners of the Oloibiri oil fields, their historical significance in the discovery of oil in West Africa has not translated into meaningful development or infrastructure for their community. They express their current situation as one of suffering, with the younger population facing unemployment and a lack of essential amenities. The absence of electricity, water, and proper roads leaves them feeling trapped and neglected while witnessing their oil resources being used to develop other regions, without benefiting their own community. Despite their vital role in the country's economy as the birthplace of the crude oil industry, Otuabagi still lacks necessities, including portable drinking water. Even after 60 years, the community continues to rely on a polluted creek for water supply. The pollution caused by oil exploration is still visible, further exacerbating their sense of marginalization. The promises made by previous administrations to develop the area and provide a sense of belonging have not been fulfilled, leaving the community in a state of disappointment and disenchantment. As expressed by Lawrence Idumesaro, the Obim V of Otuabagi, the community has not reaped the benefits it deserves despite its significant contribution to the nation's development through the crude oil industry. The neglect experienced by Otuabagi is a glaring example of how the community's historic role has not translated into tangible improvements in their quality of life. There are approximately 20 oil sites in the community, resulting in severe pollution. The environment, rivers, air quality and soil have all been adversely affected, making fishing, farming, and even bush meat hunting

unproductive. The detrimental impact of oil exploration has devastated both the environment and the community's means of sustenance [25].



Figure 1:3: The current state of the oil well spillage and effect in the community.

In this thesis, the design and analysis will be focused on a solar power pump for oil well no 17, since the oil is regarded as a stripper well with a production rate of less than 15barrel of oil per day.

#### 1.1.8 Solar energy in Nigeria and daily consumption

Nigeria's strategic geographic location in the equatorial region is a significant advantage when it comes to harnessing solar energy. The country has a well-distributed solar energy, with the northern regions receiving a higher proportion. On average, Nigeria experiences approximately 5 hours of daily sunshine, leading to a solar radiation value of about  $19.8 \text{ MJ/m}^2$ . However, the duration of sunshine varies across locations, ranging from 9 hours in the far north to 3.5 hours

towards the coast [27] and [28]. The nation receives an average of around  $7.0\text{kWh}/\text{m}^2$ , equivalent to about  $25.2\text{MJ}/\text{m}^2$  per day of solar radiation. With a device conversion efficiency of 5%, Nigeria's solar energy potential is estimated to be  $5.0 \times 10^{14}$  KJ of usable energy per year, which can be compared to the energy produced from 258.62 million barrels of oil and  $4.2 \times 10^5$  GWh of electricity annually [27].

Nigeria possesses immense solar potential due to its location in a region with abundant sunshine. According to research conducted by the Global Energy Network Institute, covering only 1% of Nigeria's geographical surface with solar collectors or modules could yield approximately  $1850 \times 10^3$  GWh of solar power each year—more than a hundred times the nation's current grid electricity consumption rate. The solar radiation map of Nigeria (Figure 1:4) indicates that the country has a solar capacity ranging from 3.5 to  $7.0\text{kW}/\text{m}^2/\text{day}$ , with an average of 4 to 7 hours of daily sunshine [27].

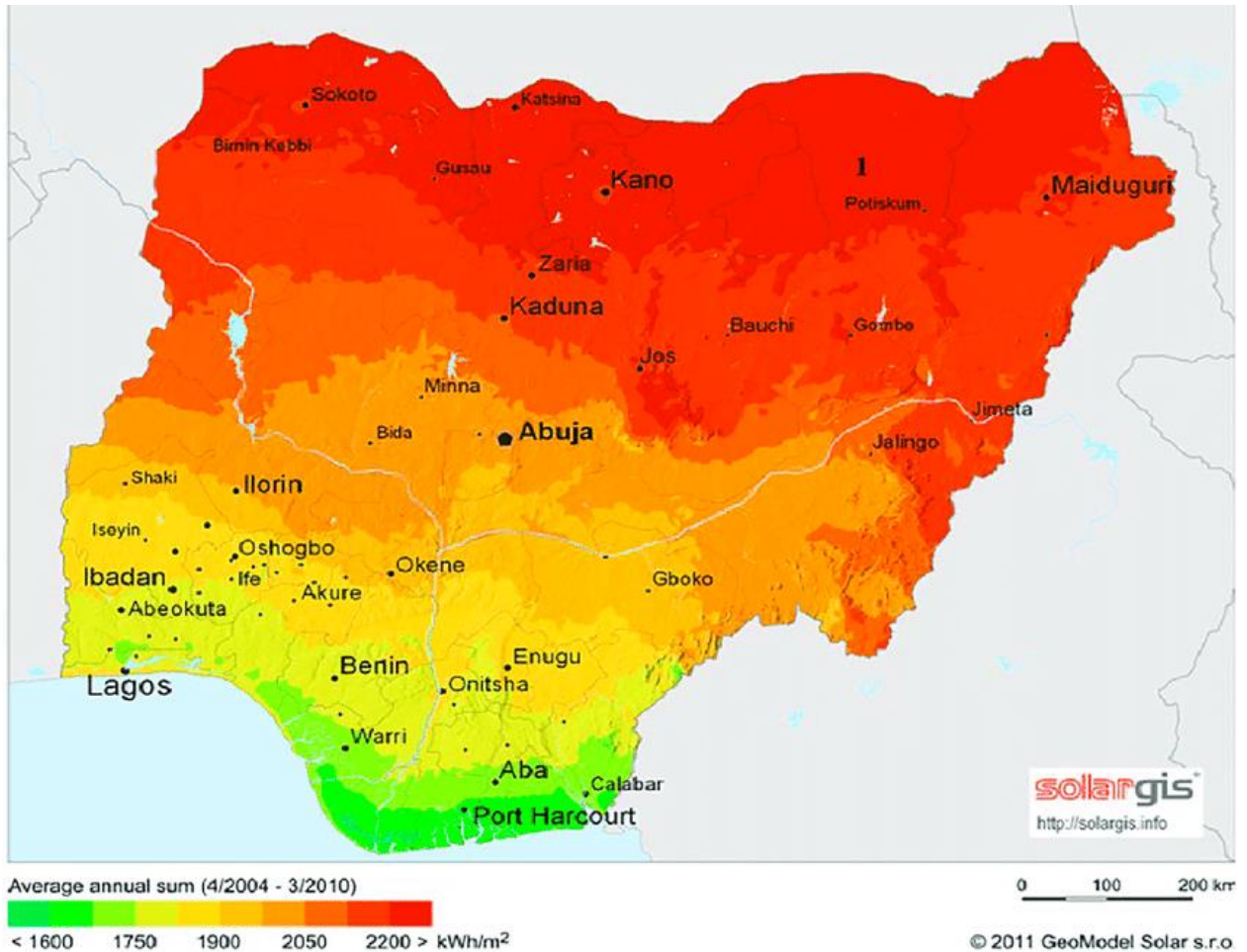


Figure 1:4: The geographical solar irradiance range in Nigeria [29]

## 1.2 Problem Statement

The implementation of renewable energy systems as alternatives for powering oil pumps in remote areas can offer reliable solution for oil spillage and can be designed to meet the required load and reduce production costs. However, in the context of the oil and gas industry, this application is currently underutilized compared to other reviewed applications. Solar-powered pumping has demonstrated effectiveness in various fields such as agriculture and water purification, successfully eliminating the reliance on fossil fuels and cutting down production expenses. Considering Nigeria's status as a major exporter of mineral resources and the limited

access to power supply to site, Oloibiri oil well, exploring and adapting similar methodologies for hydraulics like crude oil pumping will be a beneficial endeavor.

### **1.3 Research Objectives**

The primary objectives of this research and the thesis study are as follows:

1. Investigate oil well pumping in the oil and gas industry and develop a configuration for a solar-powered pumping system. This will involve calculating the load required for pumping the hydraulics considering the depth and density of the oil, and studying the mechanics of the crank pump and the piping metrics in Oloibiri oil field
2. Design the most efficient model using PVsyst and optimize the system sizing using optimization software (HOMER) under two running conditions; in a continuous flow or during the solar peak hours.
3. Implement a cost-effective real-time system monitoring solution for the oil pump's control unit, which includes spillage prevention and measurement of current, voltage, and power for the entire model using PLX DAQ. This real time data collection will further analyze the data in real time because PLX DAQ is an add on tool of Excel, which will foster better decision-making.
4. Design a remote system monitoring setup using LoRa Technology that is independent of the network system, considering the site's location. LoRa technology is a wireless communication system with long-range communication, low-power consumption, low data rate, low deployment cost, robust communication and secured data transmission.

## **1.4 Thesis Organization**

A summary of the content covered in each chapter is as follows:

Chapter One : This chapter will extensively discuss the overall working operation of the site, the solar power pump, and the site specifications required for designing the methodology that best aligns with the objectives of this thesis.

Chapter Two: This chapter will focus on optimizing stand-alone PV systems for system sizing using PVsyst. Additionally, the electrical system will be optimized using HOMER software to determine the most suitable option. The chapter will explore two case scenarios of the pumping model, including pump analysis, system efficiency, and component sizing, ensuring the overall system's cost-effectiveness and alignment with objective 1 and 2.

Chapter Three and Four: These chapters will present the implementation of real-time monitoring and measurement. A cost-effective real-time metering system will be used, involving PLX DAQ and an Excel interface to measure parameters such as current, oil level, voltage, and power. These measurements will be stored and further analyzed to fulfill objective 3 and 4.

Chapter 5: Conclusion and Future Work: This chapter will serve as the conclusion of the study, summarizing the findings and outcomes. Additionally, it will explore potential areas for future research and improvements.

## 1.5 Bibliography

- [1]G. Kuo, "When Fossil Fuels Run Out, What Then? | MAHB," MAHB, May 23, 2019. <https://mahb.stanford.edu/library-item/fossil-fuels-run/>
- [2] IPCC, "Renewable energy sources and climate change mitigation: special report of the Intergovernmental Panel on Climate Change," *Choice Reviews Online*, vol. 49, no. 11, pp. 49–630949–6309, Jul. 2012, doi: 10.5860/choice.49-6309.
- [3]S. Ericson, J. Engel-Cox, and D. Arent, "The Joint Institute for Strategic Approaches for Integrating Renewable Energy Technologies in Oil and Gas Operations," 2019. [Online]. Available: <https://www.nrel.gov/docs/fy19osti/72842.pdf>
- [4] NOAA, "How does oil impact marine life?," *Noaa.gov*, February 26, 2021. <https://oceanservice.noaa.gov/facts/oilimpacts.html/>
- [5] M. Beer, "Abandoned Wells Emerge as Massive, Largely Unmeasured Methane Risk," *The Energy Mix*, Jun. 22, 2020. <https://www.theenergymix.com/2020/06/21/abandoned-wells-emerge-as-massive-largely-unmeasured-methane-risk/#:~:text=In%20the%20U.S.%20alone%2C%20%E2%80%9Cmore%20than%203.2%20million/> (accessed Sep. 26, 2022).
- [6]"Hydrogen Sulfide - Overview | Occupational Safety and Health Administration," *www.osha.gov*. <https://www.osha.gov/hydrogen-sulfide/> (accessed Sep. 26, 2022).
- [7] M. Kang *et al.*, "Identification and characterization of high methane-emitting abandoned oil and gas wells," *Proceedings of the National Academy of Sciences*, vol. 113, no. 48, pp. 13636–13641, Nov. 2016, doi: <https://doi.org/10.1073/pnas.1605913113>.
- [8] A. Townsend-Small, T. W. Ferrara, D. R. Lyon, A. E. Fries, and B. K. Lamb, "Emissions of coalbed and natural gas methane from abandoned oil and gas wells in the United States," *Geophysical Research Letters*, vol. 43, no. 5, pp. 2283–2290, Mar. 2016, doi: <https://doi.org/10.1002/2015gl067623>.
- [9] A. R. Brandt, G. A. Heath, and D. Cooley, "Methane Leaks from Natural Gas Systems Follow Extreme Distributions," *Environmental Science & Technology*, vol. 50, no. 22, pp. 12512–12520, Oct. 2016, doi: <https://doi.org/10.1021/acs.est.6b04303>.
- [10]R. J. Davies *et al.*, "Oil and gas wells and their integrity: Implications for shale and unconventional resource exploitation," *Marine and Petroleum Geology*, vol. 56, pp. 239–254, Sep. 2014, doi: <https://doi.org/10.1016/j.marpetgeo.2014.03.001>.

- [11] L. Muehlenbachs, "A DYNAMIC MODEL OF CLEANUP: ESTIMATING SUNK COSTS IN OIL AND GAS PRODUCTION," *International Economic Review*, vol. 56, no. 1, pp. 155–185, Jan. 2015, doi: <https://doi.org/10.1111/iere.12098>.
- [12] K. C. Delhotal, F. C. de la Chesnaye, A. Gardiner, J. Bates, & A. Sankovski, (2006). "Mitigation of Methane and Nitrous Oxide Emissions from Waste", Energy and Industry. *The Energy Journal*, 27, 45–62. <http://www.jstor.org/stable/23297075>
- [13] R. O. Yusuf, Z. Z. Noor, A. H. Abba, M. A. A. Hassan, and M. F. M. Din, "Methane emission by sectors: A comprehensive review of emission sources and mitigation methods," *Renewable and Sustainable Energy Reviews*, vol. 16, no. 7, pp. 5059–5070, Sep. 2012, doi: <https://doi.org/10.1016/j.rser.2012.04.008>.
- [14] I. Karakurt, G. Aydin, and K. Aydiner, "Sources and mitigation of methane emissions by sectors: A critical review," *Renewable Energy*, vol. 39, no. 1, pp. 40–48, Mar. 2012, doi: <https://doi.org/10.1016/j.renene.2011.09.006>.
- [15] M. Kang, D. L. Mauzerall, D. Z. Ma, and M. A. Celia, "Reducing methane emissions from abandoned oil and gas wells: Strategies and costs," *Energy Policy*, vol. 132, pp. 594–601, Sep. 2019, doi: <https://doi.org/10.1016/j.enpol.2019.05.045>.
- [16] U. Jeremiah, "Reps probe oil spills, abandoned wells in Niger Delta," Vanguard News, June 30, 2022. <https://www.vanguardngr.com/2022/06/reps-probe-oil-spills-abandoned-wells-in-niger-delta/>.
- [17] S. Ugwu, "The Truth About Santa Barbara Wellhead Leak in Nembe, How Aiteo Successfully Ends Oil Spill," Energy Frontier, December 10, 2021. <https://energyfrontierng.com/the-truth-about-santa-barbara-wellhead-leak-in-nembe-how-aiteo-successfully-ends-oil-spill/> (accessed November 03, 2022).
- [18] "Reps probe oil spills at three OMLs, abandoned oil wells," *Punch Newspapers*, Jun. 29, 2022. <https://punchng.com/reps-probe-oil-spills-at-three-omls-abandoned-oil-wells/>
- [19] R. and M. ltd, "Nigeria Oil and Gas Upstream Market - Growth, Trends, COVID-19 Impact, and Forecast (2022 - 2027)," www.researchandmarkets.com. <https://www.researchandmarkets.com/reports/4828217/nigeria-oil-and-gas-upstream-market-growth/> (accessed September 02, 2022).
- [20] "Mordor intelligence," Mordorintelligence.com, 2019. <https://www.mordorintelligence.com/industry-reports/nigeria-oil-and-gas-market/>

- [21]“OLOIBIRI FIELD JANUARY 1956 - NIGERIA’S FIRST COMMERCIAL OIL - Energy Global News,” *Energy Global News*, Sep. 14, 2019. <http://www.energyglobalnews.com/oloibiri-field-january-1956-nigerias-first-commercial-oil/> (accessed Sep. 27, 2022).
- [22] Dellyson, "The Development of Petroleum In Nigeria," Dellyson Online, April 08, 2017. <https://dellysononlinecom.wordpress.com/2017/04/08/the-development-of-peroleum-in-nigeria/> (accessed September 27, 2022).
- [23] “EnergiHub | OLOIBIRI FIELD JANUARY 1956 - NIGERIA’S FIRST COMMERCIAL OIL,” *energihub.com*, Jun. 23, 2021. <https://energihub.com/article.php?slug=d1897db8/> (accessed Sep. 27, 2022).
- [24] M. Watts, “SWEET AND SOUR,” 2008. Accessed: Jul. 26, 2023. [Online]. Available: <https://geography.berkeley.edu/sites/default/files/18-watts.pdf>
- [25] S. Oyadongha and E. Idio, “60 YEARS AFTER NIGERIA’S FIRST CRUDE: Oloibiri oil dries up, natives wallow in abject poverty,” *Vanguard News*, Mar. 13, 2016. <https://www.vanguardngr.com/2016/03/60-years-after-nigerias-first-crude-oloibiri-oil-dries-up-natives-wallow-in-abject-poverty/> (accessed Sep. 27, 2022).
- [26] N. Daniel, “Where is the First Place Oil Was Discovered in Nigeria - Opera News,” *ng.opera.news*, Sep. 20, 2020. <https://ng.opera.news/ng/en/business/6c72f490c8f7a998b03081438d66b59a/> (accessed Sep. 27, 2022).
- [27] geni.org [Internet]. Global Energy Network Institute - GENI - Global electricity grid - linking renewable energy resources around the world (how is 100% renewable energy possible for Nigeria). 2014 [cited 2016 Dec 13]. Available from: <http://www.geni.org>
- [28] I. Vincent-Akpu. Renewable energy potentials of Nigeria. IAIA12 Conference Proceedings: Energy Future, The Role of Impact Assessment 32nd Annual Meeting of the International Association for Impact Assessment; 2012 May 27- June 01; Porto, Portugal. Porto: IAIA; 2012. p. 1-6
- [29] O. S. Ohunakin and B. O. Saracoglu, “A Comparative Study of Selected Multi-Criteria Decision Making Methodologies for Location Selection of Very Large Concentrated Solar Power Plants in Nigeria,” *African Journal of Science Technology Innovation and Development*, Aug. 2018, doi: 10.1080/20421338.2018.1495305.

### **Co-authorship Statement**

In the composition of this thesis, I assume the role of the primary author responsible for all the research papers. Dr. M. Tariq Iqbal, my supervisor, is acknowledged as a co-author of each of

these articles. As the lead author, my contributions encompassed conducting the majority of the research, undertaking comprehensive literature reviews, devising experimental designs, implementing hardware setups, and analyzing the obtained results for all the manuscripts. Furthermore, I authored the initial versions of the manuscripts and subsequently revised them; incorporating feedback from both, the co-author and peer reviewers during the peer review process. On the other hand, Dr. M. Tariq Iqbal played a supervisory role, overseeing the entire research process, meticulously reviewing and refining each manuscript, securing funding for the publication, providing essential research materials, contributing valuable research ideas throughout the study, and keeping the manuscripts up to date.

## Chapter 2

### DESIGN AND PERFORMANCE ANALYSIS OF AN OIL PUMP POWERED BY SOLAR FOR A REMOTE SITE IN NIGERIA

#### *Preface*

*A previous version of this manuscript underwent peer review, received acceptance, and was presented at the 2021 IEEE 31st Annual Newfoundland Electrical and Computer Engineering Conference (NECEC). The complete version has been published in the European Journal of Electrical Engineering and Computer Science (EJECE), Volume 7, Issue-1 (doi:10.24018/ejece.2023.7.1.496). As the primary author, I was responsible for conducting the majority of the research, including literature reviews, system design, implementations, and result analysis. Additionally, I took charge of drafting the initial version of the manuscript and subsequently refined it based on input from the co-author and the peer review process. Dr. M. Tariq Iqbal, the co-author, played a supervisory role in the research, securing and providing research funding, offering guidance throughout the research process, reviewing and enhancing the manuscript, and contributing valuable research ideas to shape the final manuscript.*

#### **Abstract**

Oil companies typically abandon stripper wells with production rates below 15 barrels per day because the production and maintenance cost exceed the pumping rate. Oil spillage is the primary cause of low production rates; an example of such failure is the Oloibiri oil well in Nigeria. During the peak of operation, the flow rate was 5,100 barrels per day in 1960 and was abandoned due to the declining production rate. The Oloibiri oil site has 18 drilled wells, and only the oil well 17 can be classified as stripper well. Because Nigeria has high solar irradiance and insolation, a proper PV system sizing for a solar-powered pump that should lift oil from a

depth of 3800 metres at a flow rate of 15 barrels per day is evaluated for two different running times. In that way, the solar-powered pump will be used to solve the ongoing issue of stripper oil wells by curbing oil spillage from the oil wells abandoned by these production companies and rendering a low-cost pumping system. This chapter evaluates the pump performance and completes the system design. It compares the system design to the PVsyst and HOMER sizing.

## **2.1 Introduction**

Methane (CH<sub>4</sub>) is a potent greenhouse gas that has experienced a significant increase in emissions resulting from human activities, including livestock production and fossil fuel extraction, since the onset of the industrial revolution. Compared to preindustrial levels, atmospheric concentrations of methane have more than doubled since 1750. This upward trend has raised growing concerns due to its substantial impact on global climate forcing up to the late twentieth century. There was a temporary stabilization of atmospheric methane concentrations around the turn of the new millennium, leading to hope that the previous decades' growth had ceased. Unfortunately, this period of stability was short-lived, as atmospheric methane started rising again from 2007 onwards. The precise reasons behind these fluctuations in net annual fluxes remain a subject of intense debate and ongoing research. However, it is undeniable that methane has emerged as a crucial driver of global climate forcing, and any further increase in its atmospheric concentration during the twenty-first century has the potential to undermine international efforts aimed at mitigating climate change. There are over 3.2 million abandoned oil and gas wells in the United States that are no longer operational due to various reasons. One significant environmental concern associated with these abandoned wells is the impact of stripper wells, which are oil wells producing less than 15 barrels of oil per day. According to the Energy Information Administration (EIA), around 380,000 remote oil wells in the US are in poor condition and are causing pollution to the

environment [1]. Oil spillage resulting from these abandoned wells has adverse effects on agriculture, contributes to climate change, and poses a threat to aquatic life. Despite being abandoned, these oil wells continue to contaminate aquatic environments and affect the quality of the air we breathe. Moreover, methane, a potent greenhouse gas that surpasses carbon dioxide in its heat-trapping capabilities, has been released into the atmosphere from these abandoned wells, with a total of 281 kilotons in the US [2, 3].

A recent study conducted by McGill University and published in *Environmental Science and Technology* has uncovered significant underestimation of annual methane emissions originating from abandoned oil and gas (AOG) wells in Canada and the United States. In Canada, the underestimation reaches up to 150%, while in the United States, it is approximately 20%. The study highlights that AOG wells are currently ranked as the 10th largest source of anthropogenic methane emissions in the US and the 11th largest source in Canada. As methane gas has a greater impact on global warming than carbon dioxide, especially in the short term, the researchers emphasize the need for a more comprehensive understanding of methane emissions from AOG wells. This understanding is essential for assessing the broader environmental implications and developing effective mitigation strategies to address this concern [4]. The primary method to mitigate methane emissions from numerous unplugged Abandoned Oil and Gas (AOG) wells in the United States and other regions is through well plugging. However, this approach is expensive, resulting in many wells remaining unplugged. Furthermore, plugging alone does not guarantee a significant reduction in methane emissions, as some plugged wells still exhibit high emission rates. Our analysis focuses on five options for mitigating methane emissions from high-emitting AOG wells, including both unplugged and plugged/vented gas wells. These options include plugging without gas venting, plugging with gas venting and flaring, plugging with gas venting and utilization, gas flaring only, and gas

capture/usage only. Considering the social cost of methane, which factors in air quality, climate impact, and effects on human health and ecosystems, the costs associated with these options can be justified. While savings from natural gas prices and alternative energy credits can partially offset lower plugging costs, they are inadequate to fully cover the average plugging expenses. Nevertheless, using renewable energy sources to reduce methane emissions from AOG wells proves to be a cost-effective strategy for addressing climate change, comparable to some existing greenhouse gas mitigation options. Additionally, this approach can offer co-benefits, such as protecting groundwater resources [4, 6].

Various measurements have indicated that both abandoned oil and gas (AOG) wells, whether unplugged or plugged, are releasing methane into the atmosphere. This ongoing methane emission is likely to have occurred for many decades. In Pennsylvania alone, AOG wells are estimated to contribute approximately 5-8% of the total annual human-caused methane emissions. The United States alone has over three million AOG wells, with millions more spread across different countries worldwide. Despite recently being included in the U.S. greenhouse gas emissions inventory, AOG wells have not yet been taken into account in methane emissions reduction plans [5, 6].

Hence, the primary objective is to explore cost-effective methods of mitigating methane emissions from AOG wells, and one approach is to pump out the remaining oil from these wells using renewable sources. Typically, oil companies abandon stripper wells producing below 15 barrels per day due to production and maintenance costs exceeding the production price. Low production levels are often associated with oil spillage, which is a significant contributing factor. One example of such failure can be seen in the Oloibiri oil well located in Nigeria. During its peak operation in 1960, the flow rate reached 5,100 barrels per day; however, it was ultimately abandoned due to the declining production rate. The Oloibiri oil site comprises 18

drilled wells, with only oil well 17 meeting the criteria of a stripper well. Given Nigeria's abundance of solar irradiance and insolation, this study explores the appropriate sizing of a photovoltaic (PV) system for a solar-powered pump capable of lifting oil from a depth of 3800 meters at a flow rate of 15 barrels per day. Two different running times are considered for evaluation. The chapter thoroughly assesses the pump's performance and presents a complete system design. The system design is then compared to the PVsyst and HOMER sizing to ensure its feasibility and effectiveness.

### 2.1.1 Recent Application of Solar Powered Pump in Oil Drilling

The Aztec Willson K property currently operates five wells [7]. However, due to its remote location and the expected production rate of only five barrels per day per well, the project must carefully manage costs to ensure a positive financial outcome. The high expense of installing electricity lines at the site has led to the selection of a submersible progressive cavity pump installation, which utilizes solar power and offers lower installation and maintenance costs compared to traditional pump jacks. To meet the low power requirements, DC brushless motors are chosen for the pumps. Given the site's remote location, a full remote management system is implemented, utilizing cloud-based software. This software allows for monitoring and management of all pumps through a web browser interface, accessible from any internet-connected device. Additionally, a liquid level sensor is installed to monitor and record the fluid levels in each well, transmitting the data via the cellular network.

The project outlined in [8, 9] is aimed at supporting the company's objective of reducing carbon emissions by 5% in Queensland, Australia, and the Cooper Basin by 2025. To achieve this goal, a dedicated Energy Solutions team is established to improve energy efficiency and lower emissions. The transition from crude oil to 100% renewable energy is expected to have positive environmental and economic impacts. It is anticipated that this switch will increase system

uptime and production, decrease fuel usage, and eliminate reliance on potentially unreliable fuel generators. Moreover, maintenance and operational costs associated with fuel trucking will be reduced. The system utilizes high-efficiency photovoltaic (PV) arrays to generate DC power, which is then converted to AC electricity by an inverter to power the beam pump. Any surplus energy is stored in batteries, and when the beam pump's load exceeds the PV generation capacity, the batteries release stored energy through the inverters to power the pump. A remote-control system is implemented to monitor and regulate the battery charging and discharging process. Sizing the units takes into consideration the cyclic load of the beam pumps, which varies with the pump speed and up-and-down strokes, to ensure the load requirements are met effectively.

The solar-powered oil pumping systems offered by Solar Lighting International consist of a Crank Rod Pump designed specifically for shallow and low-flow oil wells, particularly those located in rural areas [10]. Unlike conventional linear rod pumps, the solar-powered crank rod system eliminates the need for complex mechanical components. It converts variable-speed rotary motion into vertically reciprocating motion, powering the rod string through a primary crank mechanism. The system is compact, lightweight, and easy to install and relocate, directly mounting onto the wellhead. Operating at low speeds, the crank rod pump allows low-volume wells to continue production without shutdown, making it an ideal option for refurbishing older wells. Its portability facilitates temporary installations or reserve demonstrations, as it can be transported from one well to another.

The sucker-rod pump control system optimizes production while safeguarding the pumping system. Notably, the crank rod pump system's unique ability to run on solar power makes it a versatile and environmentally friendly solution for areas lacking access to the power grid. The power demand is balanced through flywheel energy storage, and power usage control ensures

the complete output of the solar collecting array is always utilized, enabling the device to pump various fluids effectively. In the existing literature review, only a few studies on solar-powered oil pumps were found, and none of them provided comprehensive design details and methodologies used. This chapter presents a case study for a site in Nigeria, offering a thorough design, system sizing, and analysis of the proposed system.

Oil and gas companies face significant challenges during the production process, including issues such as water and sand filling the wellbore, corrosion of steel pipes, and challenging working conditions. To address these operational difficulties and enhance production efficiency, the industry has adopted a creative approach of adding chemicals to the wellbore. These chemicals can help mitigate the negative impacts of the operational environment and resolve various production-related issues. One solution used by the industry is the use of corrosion preventers, which extend the lifespan of steel tubing used to transport the oil and gas stream from the subsurface reservoir to the surface. Additionally, pumps with diaphragms offer a chemically resistant and long-lasting option for oilfield chemical injection. One such solution is a solar-powered diaphragm pump that utilizes a diaphragm metering system, a well-established technology. The diaphragm-metering pump combines a sealed, brushless, non-sparking direct current (DC) motor with a plug-in timer to ensure precise and accurate injection rates. This timer is powered by a 12-volt DC power source, often a battery with a solar panel [11].

Tests conducted in [11] on the solar powered pump have demonstrated its ability to maintain a remarkably consistent injection rate within a 95 percent confidence interval for the pressure range of 300 to 1,200 psi (21 to 83 bar). As a result, the pump allows operators to inject chemicals in precise quantities, reducing the tendency to use excessive amounts of chemicals and leading to significant cost savings. By employing this solar-powered diaphragm pump, oil

and gas companies can effectively address production challenges and enhance their operational efficiency. To the dismay of some environmentalists, Chevron Corp. has figured out a way to exploit one of the state's clean-energy initiatives to reduce the cost of pumping oil. The 7,981 barrel-per-day Lost Hills oil field operated by Chevron has been using solar energy to power oil pumps since April 2020, the firm claims. The 29-megawatt facility, owned and run by Sun Power Corp. in San Jose, is intended to supply the field with 80% of its power [12].

### 2.1.2 Upstream: Renewable Integration in Oil and Gas Production

In the upstream operations of the oil and gas industry, the integration of renewable energy sources can lead to several benefits, including reducing fuel consumption and lowering maintenance expenses. Moreover, renewable energy can contribute to lower noise levels, reduced pollution, and improved safety. Different stages of an oil field's process cycle can utilize various renewable technologies, which can be categorized into three, manufacturing phase:

Primary recovery: In this phase, the well pressure alone is sufficient for oil and gas extraction. To enhance productivity, artificial lift techniques like rod pumps and electric submersible pumps (ESPs) are often employed. Primary recovery allows for the extraction of approximately 5%–15% of the total reserves [13]. In the Secondary recovery stage the reservoir pressures decrease, the production enters the secondary recovery phase. To increase the reservoir's pressure, gas or injection fluids are used. Secondary recovery enables the extraction of an additional 10%–20% of the remaining reserves [14]. While the last stage, which is the Tertiary recovery, also known as enhanced oil recovery. The tertiary recovery involves implementing various techniques to further boost output. Examples include chemical injection, in-situ combustion, steam injection, and hydraulic fracturing. During tertiary recovery, it is possible to retrieve up to 20% more of the original reserves [15]. It is important to note that different

wells within a field may be in different production phases at any given time, and not all fields experience all three phases simultaneously. However, this distinction provides a valuable conceptual framework for understanding the general production phases and potential integration points for renewable energy generation technologies.

### 2.1.3 Electric pumps in the oil and gas production

Electric submersible pump (ESP) systems are widely recognized in the oil and gas industry as a dependable artificial lift method for efficiently pumping production fluids to the surface. ESPs have proven to be highly effective in wells with characteristics such as low bottom hole pressure, low gas/oil ratio, low bubble point, high water cut, or low API gravity fluids. Over the past several years, ESP technology has gained a reputation as a cost-effective and low-maintenance alternative to vertical turbine, split case, and positive displacement pumps in various fluid movement surface applications within the petroleum sector [16].

#### Artificial lift technologies

Are used to enhance the flow of liquids (e.g., crude oil or water with some gas content) to the surface of a production well. This can be achieved through three main methods: (1) using a mechanical device like a pump inside the well; (2) employing high-pressure gas to reduce the weight of the liquid/gas mixture; or (3) utilizing velocity strings to improve the well's lift efficiency. Artificial lift systems are necessary in wells where the reservoir's pressure is insufficient to bring the liquid to the surface. Additionally, these systems are occasionally employed in flowing wells to increase the natural flow rate. More than 60% of operating oil wells require some form of artificial lift technology to pump recoverable oil, especially from abandoned wells with low oil production. Some of the artificial lift methods used include plunger lift, beam/sucker rod pumps, gas lift, progressive cavity pumps (PCP), and electric submersible pumps.

**Plunger lift**, for instance, is commonly used in gas wells to extract relatively small amounts of liquid. It involves a mechanical linkage between the gas and generated liquids using a plunger-lift device. The movement of a free-traveling piston (plunger) from the bottom of the well to the surface forces the liquids to the surface using the wells own energy for lift. This mechanical contact enhances the well's lifting efficiency by preventing liquid fallback and increasing inflow when average flowing bottom hole pressure decreases. During well shut-in periods, formation gas is often stored in the casing annulus to facilitate plunger travel. As the well is opened and the tubing pressure drops, the stored casing gas pushes the plunger to the surface, and this process is repeated multiple times a day.

## **2.2 Site Characteristics – Oloibiri Oil Well 17 Field**

The Oloibiri oilfield is located in Bayelsa State, Nigeria; the 13.75km<sup>2</sup> oil site is under a marsh of Oil Mining License OML 29. The discovery well Oilwell 1 depth is 108 feet and was founded on August 3, 1955. On average, the field produced five thousand hundred barrels of oil daily for the first year. After that, production increased as new wells were drilled and put into use, reaching peak production in 1964, with eighteen oil-producing wells. The field produces heavy oil with an API rating of 20.6. The oilfield produced over 20 million barrels of oil during its 20-year life. When oil production finally ended in 1978, the field was shut down the following year. The Oloibiri oilfield-17 was neglected without any possibility of recovering the remnant still present on the site. After declining production, the Oloibiri-17 appraisal well was drilled to a measured depth of 12,520 feet because the pump rate from the previous appraisals was drastically low. The oil spillage from Oloibiri caused most oil wells to dry up. At that time, the field's output decreased less than its peak production period. Only oil well 17 was considered a stripper well with a production rate of under 15 barrels per day .Since oil well

No. 17 is considered a stripper well with a production rate of about 15 barrels per day, this chapter will design and analyze a solar power pump.

## 2.3 System Design Calculation

### 2.3.1 Site Description

The required flow rate and head determine the selection of a suitable pump. For this case, the pumping level was set at a depth of 3800m to prevent any damage to the pump caused by potential foreign bodies, such as sediments or sand present in the crude oil. The oil well's total depth is 3816m, with a total dynamic head of approximately 3820m and a static water level of 3710m from the ground. The daily oil production at this site amounts to about 15 barrels, which is equivalent to  $2.4 \text{ m}^3 / \text{day}$ . Under these specified conditions, we will analyze and compare the performance of the two pumping systems.

Condition A: the system runs for 5 hours daily when it is sunny. Flow rate per second =  $\frac{2.4}{5 \times 60 \times 60}$   
=  $0.00013 \text{ m}^3 / \text{s}$  ( $0.5 \text{ m}^3 / \text{h}$ ).

Condition B; system is running for 24 hours, irrespective of solar irradiance, the flow rate per second =  $\frac{2.4}{24 \times 60 \times 60} = 0.000027 \text{ m}^3 / \text{s}$  ( $0.1 \text{ m}^3 / \text{h}$ ).

$\text{TDH} = 3816 + [(0.9 \times 1) + 5] \times 0.2 = 3817\text{m}$ . However, 3820m is the estimation for the total dynamic head.

### 2.3.2 Solar Irradiance of the Site.

The most suitable application of renewable energy technology in Nigeria would be the incorporation of solar energy, given the country's abundant solar irradiance and extended periods of solar insolation. The solar irradiance of the specific location was assessed using the

Homer software. The solar resources at the site are depicted in Figure 2.1, as obtained from the HOMERpro software.

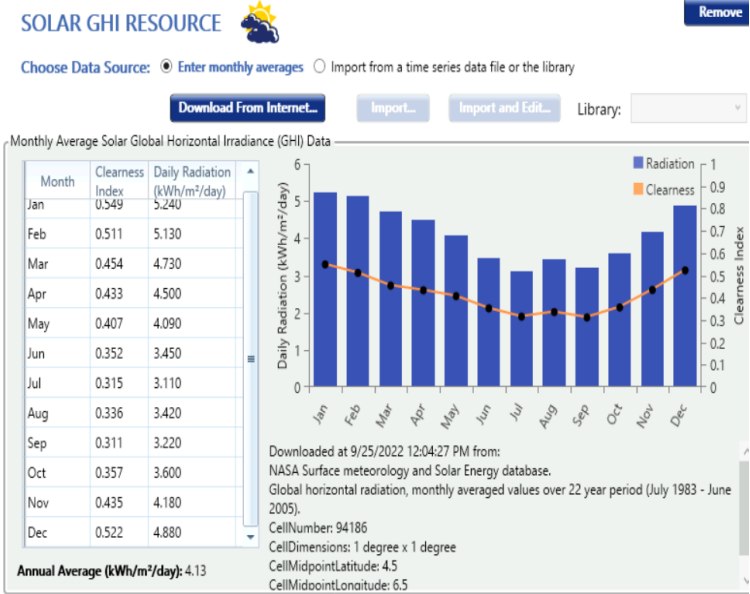


Figure 2:1: Solar Global Horizontal Irradiance for Oloibiri, Nigeria (HOMER)

In Oloibiri, Nigeria, the peak monthly average solar irradiation is observed in January, whereas the lowest occurs in July. The region experiences an annual average solar radiation of 4.13 kWh/m<sup>2</sup>/day .The solar day is characterized by varying sunshine durations, ranging from 5 to 9 hours, indicating the duration of sunlight received in that area.

2.3.3 Pump Sizing

For the expectation of the pump sizing, it can be calculated using hydraulic power over the efficiency for a simple calculation.

Mathematically,

Shaft power

$$\frac{\text{hydraulic power}}{\text{efficiency}} \quad (2)$$

Also, hydraulic power

$$\rho \times g \times H \times Q \quad (3)$$

Where,

$\rho$  is the density

H is the total dynamic head in m,

Q is the flow rate in  $m^3/s$ , and

g is the gravitational constant in  $m/s^2$ .

Assuming a pump efficiency of 30% for the basic calculations, it is noted that the heavy crude oil's density is  $925kg/m^3$ . However, due to the well's depth and high pressure at the bottom level, the density becomes nearly equivalent to that of water, which is  $1000kg/m^3$ . Since the oil will be heated at that depth, its viscosity is low. As demonstrated earlier, for condition A, where the system operates for 5 hours per day, the total dynamic head is 3820 m, with a maximum flow rate of  $0.00013m^3/s$ . With the efficiency assumption, the calculated hydraulic power is 4,506 W, and a shaft power of 15 kW can deliver the required amount of oil.

For condition B, which represents a system operating continuously with a maximum flow rate of  $0.000027m^3/s$ , the calculated hydraulic power is 934.96 W. With the hand calculation's 30% efficiency, a shaft power of 3.11 kW is sufficient to deliver the required amount of oil. Although the above calculation provides a preliminary idea of the system design, a comprehensive system sizing is conducted using solar energy software.

### 2.4 Solar Pump Design by Pvsyst

PVsyst software is employed to accurately determine the appropriate size of the solar pump, tailored to match the specific requirements of the site, which includes parameters such as the lower dynamic, pump level, borehole diameter, static level, and drawdown. Given the depth of the well, the density of the oil is equivalent to that of water. The system design in Figure 5 necessitates the following oil well specifications. The customized delivery pipe material is made of medium-pressure seamless steel, with an inner diameter of 200mm and an outer diameter of 217mm.

#### 2.4.1 Pump Sizing for a Running Time of 5 hours/day

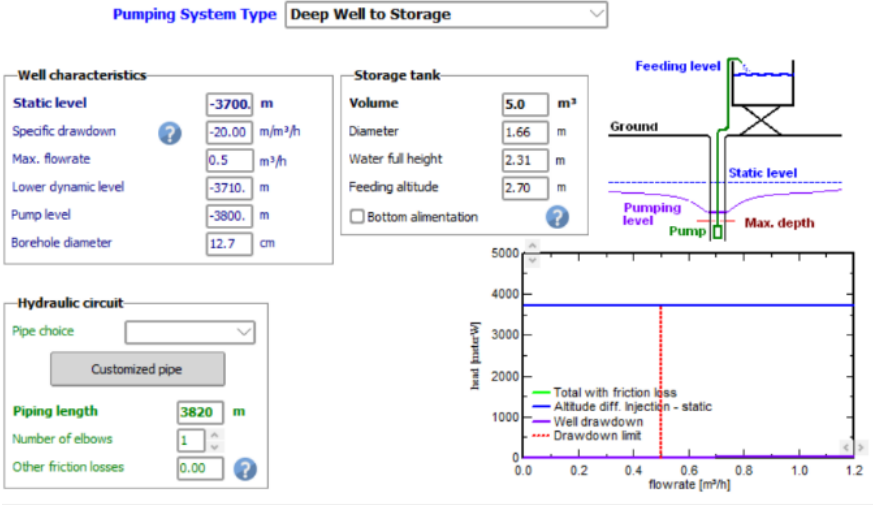


Figure 2:2: Input parameter for the system in PVsyst

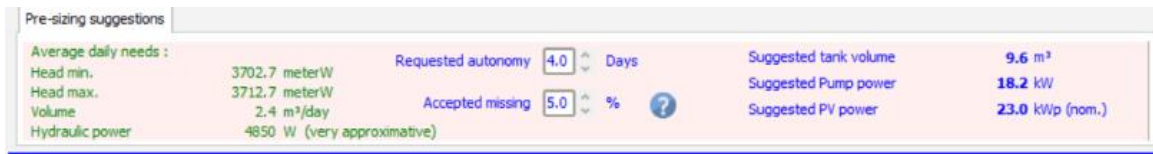


Figure 2:3: PVsyst system sizing Suggestion

As observed in Figure 2.3, PVsyst software analyzed the system sizing and determined that the oil has a minimum head of 3702.7 meters and a maximum head of 3712.7 meters. The hydraulic power was calculated to be 4850W, and PVsyst recommended a pump power of 18.2kW and a PV system capacity of 23kWp.

#### 2.4.2 Pump Sizing for continuous running time (non-stop)

PVsyst software provided similar pump parameters to the other running conditions. When a flow rate of  $0.000027m^3/s$  was input, as depicted in Figure 5, PVsyst recommended a pump power of 18.5 kW, a PV power of 18.5 kW, and a tank storage capacity of  $9.6m^3$  to meet the load demand for continuous operation, as illustrated in Figure 2.4



Figure 2:4: PVsyst system sizing Suggestion

## 2.5 PV Sizing by Homerpro Software

Since PVsyst suggests sizing the system at approximately 18.2 kW and 18.5 kW for the 2 conditions, an additional 1.8 kW is added to accommodate extra energy needs for system monitoring and lighting. However, to precisely determine the optimal PV rating capable of handling the required electrical load for both the 5-hours daily and continuous flow operating periods, the HOMERPro software will be used. It is important to note that this is one limitation of PVsyst, as it may not provide the exact sizing required for the system under all conditions.



Figure 2:5: Condition a Load Picture

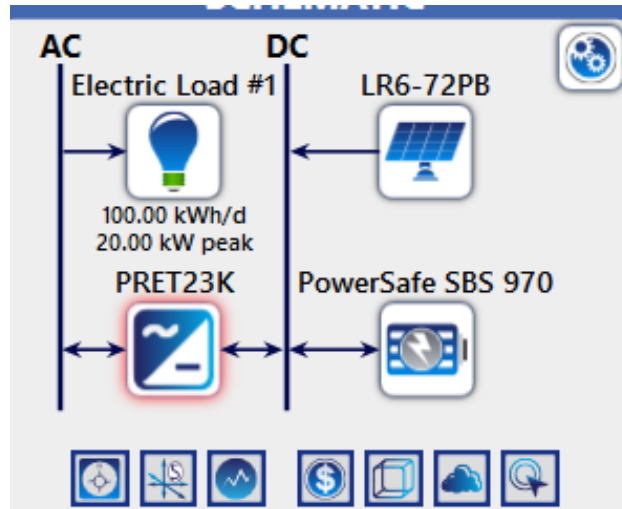


Figure 2:6: System Sizing Architecture

The system is intended to be used fully during its operating window of 11 am to 4 pm when solar irradiance is at its highest. Figures 8 and 9 above show the system design for 5 hours of running time in HOMERpro.

For the system design, a 22.3kW converter, a 50kW of 370W 24V Solar panel, 40 (970Ah, 12V) batteries, and One string of 20 batteries has a DC bus voltage of 240V is used. Figure 10 shows the renewable fraction of 100%, 33.9% of the electricity being in excess, and 0.08% of the load being unmet and 0.09% of the capacity shortage.

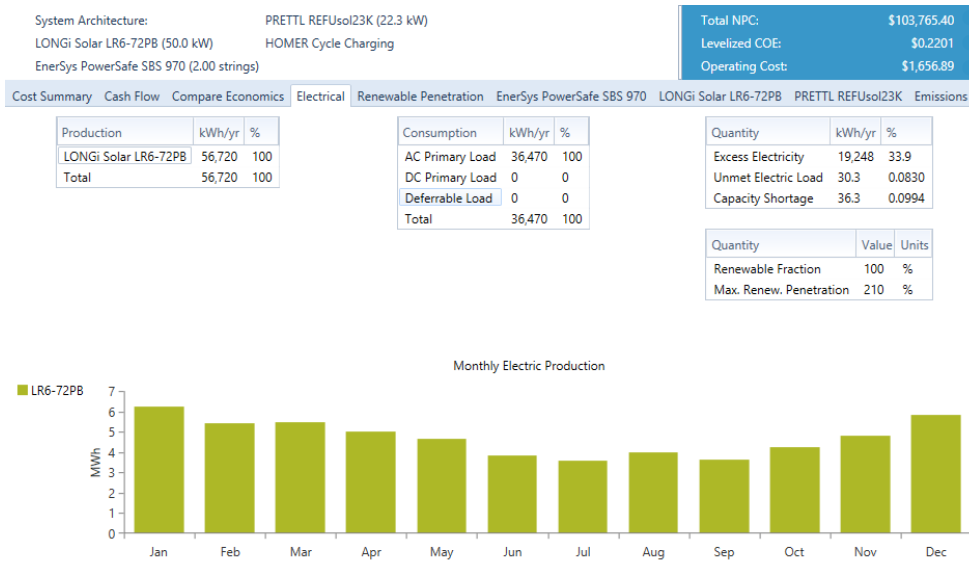


Figure 2:7: Simulation result details

- PV sizing for the system that operates continuously under the same system component as under condition A.

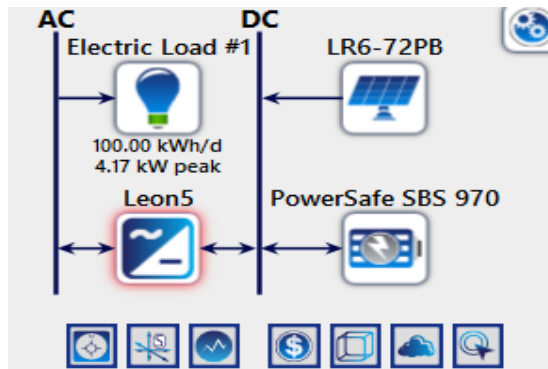


Figure 2:8: System Sizing Architecture

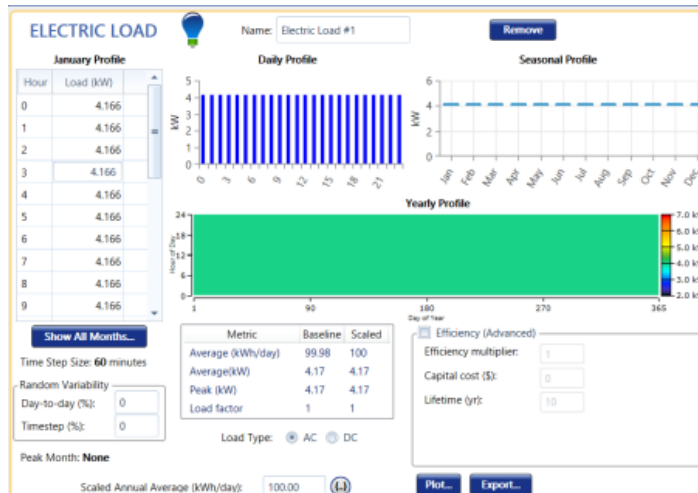


Figure 2:9: Condition B Load profile

The system design includes a 5.88 kW converter, 40 (970Ah, 12V) batteries, and 54.9 kW of 370W, 24V Solar panels. Figure 13 depicts a 100% renewable percentage, with 38% of electricity being in excess, 0.8% of the electric load being unmet and 0.09% of capacity being short. The 240V DC bus voltage, or twenty 12V battery banks connected in series, was set.

The system's 24-hour operation results in a higher PV capacity and surplus electricity when compared to condition A.

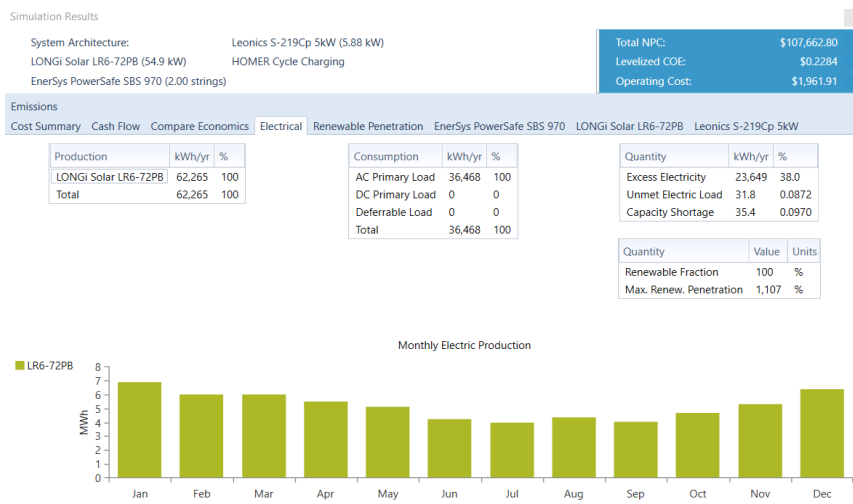


Figure 2:10: Simulation result details

## 2.5.1 PV Panel and Battery Performance

The penetration level met all load requirements by 156%, as shown in figure 14. However, the battery's internal system characteristics reveal that the state of charge began to decrease significantly in August. Figure 15 shows that in September, this reduction ended for a system running for 5 hours.



Figure 2:11: Renewable Penetration details

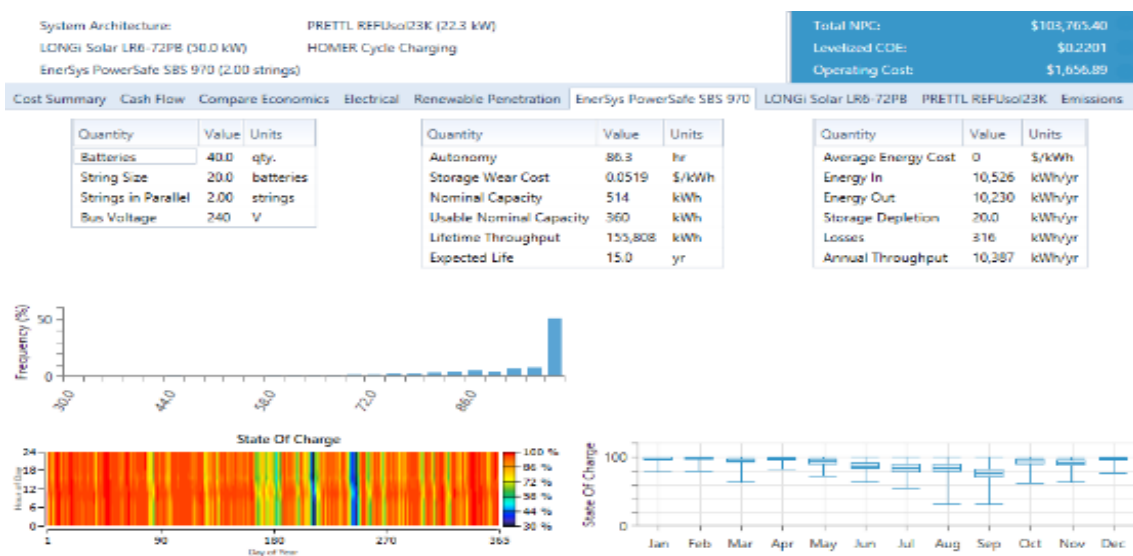


Figure 2:12: Battery performance details

Even though the specifics of renewable penetration are the same in both situations, the battery's internal system characteristics demonstrate that the state of charge rapidly depletes in August. Figure 16 shows that in September, this decline ended.



Figure 2:13: Battery performance details for 24 hours running time

## 2.6 System Performance

The oil well is too deep for PVsyst to evaluate the pump dynamics. As a result, the maximum head is set at 100 metres, and the static head and dynamic level are set at the same level position as the site characteristics. In order to account for the TDH of 3820m, 38.2 to mimic the system's performance fully will multiply each result. The pump is specified based on the requirements of the static head and the pump power.

For the system evaluation for condition A, a 1.4kW Grundfos Solflex DC pump with a brushless DC motor with a maximum power of 1400 W, 120 V, and 3.8 A is used. The pump power for condition A is 422W by PVsyst. Figure 17's main result demonstrates that the pump performance efficiency is 37.9%, and the overall system efficiency is 11.4%.



Figure 2:14: Pre-sizing parameter, simulation parameters and results

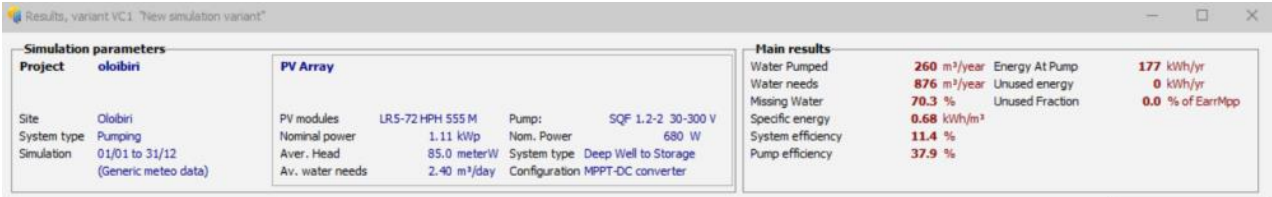


Figure 2:15: Pre-sizing parameter, simulation parameters and results

For condition B, the pump power is 328 W. Lorentz DC pump with a brushless DC motor with a maximum power of 600 W, 140 V, and 3.1 A is used for system evaluation. Figure 18 indicates that the pump efficiency is 11.4%, overall efficiency is 5.6%, and there is 97.7% missing oil.

Pre-sizing suggestions			
Average daily needs :		Requested autonomy	4.0 Days
Head min.	87.7 meterW	Accepted missing	5.0 %
Head max.	89.7 meterW		
Volume	2.4 m <sup>3</sup> /day		
Hydraulic power	116 W (very approximative)		
		Suggested tank volume	9.6 m <sup>3</sup>
		Suggested Pump power	328 W
		Suggested PV power	415 Wp (nom.)

Figure 2:16: Pre-sizing parameter, simulation parameters and results.

Simulation parameters				Main results			
Project	New Project ony	PV Array		Water Pumped	20 m <sup>3</sup> /year	Energy At Pump	43 kWh/yr
Site	Olobiri	PV modules	LR5-72HPH 555 M G2	Water needs	876 m <sup>3</sup> /year	Unused energy	0 kWh/yr
System type	Pumping	Nominal power	0.56 kWp	Missing Water	97.7 %	Unused fraction	0.0 % of EarrMpp
Simulation	01/01 to 31/12 (Generic meteo data)	Pump:	PS-1800 HR-07	Specific energy	2.13 kWh/m <sup>3</sup>		
		Nom. Power	600 W	System efficiency	5.6 %		
		Aver. Head	85.0 meterW	Pump efficiency	11.4 %		
		Av. water needs	2.40 m <sup>3</sup> /day				
			System type: Deep Well to Storage				
			Configuration: MPPT-DC converter				

Figure 2:17: Pre-sizing parameter, simulation parameters and results.

Figure 2:17 represents a system size for a 100 m depth along with the flow rate for a 5-hour running time. Recall that 38.2 will multiply every result. Therefore, the PV power is 20.36kWp, and the pump power is 16.12kW, with losses not considered.

Figure 2:18 represents a system size for a 100 m depth along with a continuous flow. Recall that 38.2 in figure 18 will multiply every result. Therefore, the PV power is 15.9kWp, and the pump power is 12.5kW with losses not taken into account.

According to the above design and analysis, the design sizing for both systems is the same, but the system's efficiency when running for five hours is best suited for the location. The system consists of a 22.3kW converter, 40 (970Ah, 12V) batteries, and a 50 kW of 370W 24V Solar panel. Figure 19 offers a thorough system design diagram that will run for five hours.

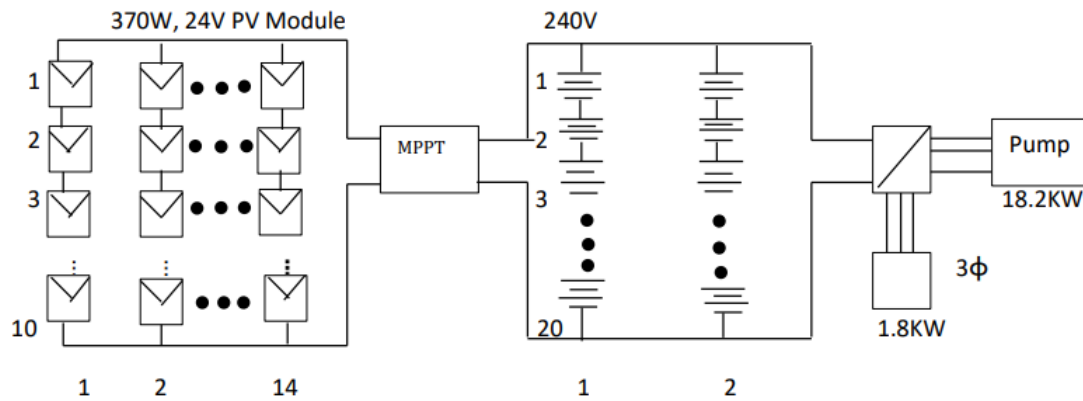


Figure 2:18: Detailed System Design Diagram

## 2.7 Conclusion

The environmental effects of an abandoned well with a low production rate are catastrophic. Alternative and cost-effective technology, like the solar-powered pump, is an easy way to address this issue because of how expensive for oil companies to minimize the impact by pumping the leftovers. For Olobiri oil well 17, this Chapter proposed intensive system sizing. The PVsyst made recommendations for the pump's size, and the software's performance was assessed by simulating an oil depth to account for the site's specifications. According to the software, the system and pump efficiencies are 11.4% and 37.9% for 5 hours of running time. Also, 5% of system efficiency and 11% of pump efficiency were indicated when there was a continuous flow. To properly size the PV setup in HOMERpro, the overall load of the entire power system was considered. According to the PVsyst Suggestion, the software recommended a PV unit of 50kW and 54.9kW for working conditions with exact size specifications for batteries. However, the system running for 5 hours is more efficient when compared.

## 2.8 Bibliography

- [1] "Stripper Oil Wells," thenowcorporation.weebly.com.  
<https://thenowcorporation.weebly.com/stripper-oil-wells.html#:~:text=American%20energy%20is%20increasingly%20supplied%20by%20what%20we/>  
(accessed September 26, 2022).
- [2] A. Moseman and J. Trancik, "Why do we compare methane to carbon dioxide over a 100-year timeframe? Are we underrating the importance of methane emissions?," MIT Climate Portal, June 28, 2021.
- [3] M. Beer, "Abandoned Wells Emerge as Massive, Largely Unmeasured Methane Risk," The Energy Mix, June 22, 2020. <https://www.theenergymix.com/2020/06/21/abandoned-wells-emerge-as-massive-largely-unmeasured-methane-risk/#:~:text=In%20the%20U.S.%20alone%2C%20%E2%80%9Cmore%20than%203.2%20million/>  
(accessed September 26, 2022).
- [4] k.Gombay, "Methane emissions from abandoned oil and gas wells underestimated," *Newsroom*, Jan. 21, 2021. <https://www.mcgill.ca/newsroom/channels/news/methane-emissions-abandoned-oil-and-gas-wells-underestimated-327816> (accessed Jul. 27, 2023).
- [5] E. D. Lebel *et al.*, "Methane Emissions from Abandoned Oil and Gas Wells in California," *Environmental Science & Technology*, vol. 54, no. 22, pp. 14617–14626, Oct. 2020, doi: <https://doi.org/10.1021/acs.est.0c05279>.
- [6] J. P. Williams, A. Regehr, and M. Kang, "Methane Emissions from Abandoned Oil and Gas Wells in Canada and the United States," *Environmental Science & Technology*, vol. 55, no. 1, pp. 563–570, Dec. 2020, doi: <https://doi.org/10.1021/acs.est.0c04265>.
- [7] "Oil pumping using low energy pumps and solar power in the United States," Lorentz.de, Mar.2018. [https://partnernet.lorentz.de/files/lorentz\\_casestudy\\_oil\\_texsec\\_us.pdf](https://partnernet.lorentz.de/files/lorentz_casestudy_oil_texsec_us.pdf) (accessed September 27, 2022).

- [8] L. Cella, "Converting crude oil beam pumps to solar power in the Cooper Basin," *Pump Industry Magazine*, July 14, 2020. <https://www.pumpindustry.com.au/converting-crude-oil-beam-pumps-to-solar-power-in-the-cooper-basin/> (accessed September 02, 2022).
- [9] "Conversion of Remote Crude Oil Beam Pumps to Solar & Battery Final Report," Australian Renewable Energy Agency. <https://arena.gov.au/knowledge-bank/final-report-conversion-of-remote-crude-oil-beam-pumps-to-solar-battery/> (accessed September 02, 2022).
- [10] Solar Lighting International, "Solar Oil Pump | Solar Oil Well Pumping," *Solar Lighting International*, 2020. <https://www.solarlightingintl.com/solar-oil-well-pumping> (accessed Jul. 27, 2023).
- [11] T. O'Donnell, "Solar-Powered Pumps Increase Oilfield Profitability," *Pumps and Systems Magazine*, Oct. 15, 2014. <https://www.pumpsandsystems.com/solar-powered-pumps-increase-oilfield-profitability>
- [12] "Powering an Oil Field: Leave it to the Sun," *chevron.com*, May 05, 2022. <https://www.chevron.com/newsroom/2022/q2/powering-an-oil-field-leave-it-to-the-sun> (accessed Jul. 27, 2023).
- [13] A. Abromova, A. Vladimir, S. Kuleshov, and E. Timashev. "Analysis of the Modern Methods for Enhanced Oil Recovery." In *Energy Science and Technology*, 2014. 118- 148P.
- [14] K. Veld, and P. Owen. 2010. "The Economics of Enhanced oil Recovery: Estimating Incremental Oil Supply and CO2 Demand in the Powder River Basin." *Energy Journal* 31 (3): 31-55.
- [15] S. Ericson, J. Engel-Cox, and D. Arent, "The Joint Institute for Strategic Approaches for Integrating Renewable Energy Technologies in Oil and Gas Operations," 2019. Available: <https://www.nrel.gov/docs/fy19osti/72842.pdf>
- [16] S. Breit, N. Ferrier, and Wood Group ESP, Inc., "Electric Submersible Pumps in the Oil and Gas Industry," *Pumps and Systems Magazine*, Dec. 17, 2011. <https://www.pumpsandsystems.com/electric-submersible-pumps-oil-and-gas-industry>

## Chapter 3

### SYSTEM MONITORING AND DATA LOGGING USING PLX-DAQ FOR SOLAR-POWERED OIL WELL

#### *Preface*

*A version of this manuscript has been published in 2023 IEEE 13<sup>th</sup> Annual Computing and Communication Workshop and Conference (CCWC) The paper has also been published on IEEE Xplore Database as a part of the IEEE CCWC 2023 conference proceedings (doi: 10.1109/CCWC57344.2023.10099099)I am the primary author, and I carried out most of the research work, performed the literature reviews, carried out the system design, modeling, and analysis of the results. I also prepared the first draft of the manuscript and subsequently revised the final manuscript based on the feedback from the co-author and the peer review process. The Co-author, Dr. M. Tariq Iqbal, supervised the research, acquired, and made available the research funding, provided the research guide, reviewed and corrected the manuscript, and contributed research ideas in the actualization of the manuscript.*

#### *Abstract*

Solar-powered systems require real-time monitoring because the rapid environmental change affects the system with no specifics when such occurrences will happen. The systems rely solely on the amount of solar irradiance, which can affect the overall working performance. This paper introduces cost-effective instrumentation and measurement of the entire solar system essential for remote areas. The instrumentation method described in this paper offers a low-cost method for real-time monitoring of the voltage of the battery bank, current from the PV, AC from the converter and oil well control. An Arduino board serves as the foundation for the system design. A low-cost current, voltage and float switch sensors are used for the acquisition, and data are

presented in Excel using the PLX-DAQ data acquisition Excel Macro, which enables the communication between the Arduino U.N.O. board's ATmega328 microcontroller and the computer via the UART bus.

### **3.1 Introduction**

The solar-powered pumping unit must be monitored to evaluate the operating performance of the overall system. The manual data-gathering approach is labour-intensive, using measuring tools like multimeters. Due to the quick change in ambient conditions, getting readings accurately at any rapid change is challenging. As a result, sensor-based data acquisition (DAQ) systems are required and offer quick data precision in real-time in place of manual measurement for monitoring the PV systems' operation and storing the data. Monitoring the PV system parameters helps guarantee system health and provides data on energy flow from the PV panel. The voltage, current flow, and temperature analysis of various defects that may arise can associate with energy loss. Hence, lower data acquisition costs should be incorporated for system monitoring to ensure the PV outperforms [1]. In order to prevent the effects of shading from the sun, PV systems have to be installed in open areas with direct sun exposure. The ambient environmental change, such as solar irradiance, temperature, humidity, wind speed and direction, and dust accumulation, significantly influences the energy generated by PV systems [2]. The PV converts about 10%-16% of solar energy into electricity; the heat generated by solar radiation, the PV panel temperature rises dramatically, and the PV efficiency decreases [3] influence this. In this Chapter, the system monitoring will cover the voltage of the battery bank, current from the PV, AC from the converter and oil well control monitoring. In this chapter will discuss how solar-powered systems require real-time monitoring because any rapid environmental change affects the system without specifics on when such occurrences will

happen. The systems rely solely on the amount of solar irradiance, which can affect the overall working performance. This Chapter introduces cost-effective instrumentation and measurement of the entire solar system essential for remote areas. The instrumentation method described in this paper offers a low-cost method for real-time monitoring of the voltage of the battery bank, current from the PV, AC current from the converter and oil well control. The Arduino board serves as the foundation for the system design. A low-cost current, voltage and float switch sensors are used for the acquisition, and data are presented in Excel. The PLX-DAQ, a data acquisition tool, which enables the communication between the Arduino UNO embedded with ATmega328 microcontroller, is used for logging data and presenting it in Excel.

### **3.2 Literature Review**

The battery monitoring system in [4] uses Bluetooth technology, which is made up of a lead-acid battery, an Arduino microcontroller, a voltage divider circuit, a current sensor, a Bluetooth module, and a laptop computer. The author employs a wireless communication system for monitoring by connecting a Hall Effect sensor with the battery that detects the current flow. When the input terminals of the voltage divider circuit are connected to the battery terminals, it can determine the battery's output voltage. The battery's voltage and current values are translated and delivered to the Bluetooth module via the microcontroller's serial port. The HC-05 Bluetooth module was created for serial wireless setup and is part of the serial port protocol. Microsoft Excel is integrated with the Parallax Data Acquisition (PLX-DAQ) software application, which collects data from a microcontroller connected to it and stores it in the Excel sheet as it comes in. PLX-DAQ can use Microsoft Excel to plot the graph as the data comes in. The data collection in [5] is designed to measure water flow. In this study, an electronic system, which acts as a simulator, is constructed to measure the flow in water, using the HC-SR04

ultrasonic sensor and DHT 11 for humidity sensing with Arduino UNO as the microcontroller. The LCD displays the data processed by the Arduino, and Microsoft Excel delivers the data reading-using PLXDAQ, where it can be immediately monitored and displayed for the user. The digitalization of data and information on water flow in the dam design can be readily observed and supplied to monitoring stations. The study of measuring water flow in the industrial sector, agricultural irrigation, and other water management that needs data acquisition for the water flow is solved by the findings of this study and measured in real-time.

The PLX DAQ software enables affordable and accessible data acquisition based on Arduino. Recent advancements in microcontroller-based DAQ provide an excellent way to ensure proper operation on photovoltaic systems. On the other hand, commercial DAQ data loggers are extremely expensive, need extra expertise, and require a constant connection to an external power source [6]. The primary objective of this project in [7] is to develop and construct an affordable DAQ for tracking the PV system parameters of the Solar Home System (SHS) prototype. The DAQ device is built on the Arduino Mega board's ATmega 2560 chip microprocessor and has real-time data recording, low power consumption, and open-source software. Analysis of the PV system performance, whose parameters data are collected in PLX DAQ was achieved [7]. In this paper, we present a low cost monitoring system for a solar oil pumping system. The proposed system will be useful for small remote stripper oil wells.

### **3.3 Methodology**

This real-time instrumentation system can measure the oil level and how the energy flows from the PV passing through the schematics by measuring the voltage from the battery, current from the inverter and PV and power, as shown in figure 1. The system sizing in figure1 has been

done in the previous study in [8]. PLX-DAQ (Parallax Data Acquisition), a plug-in, will be used for logging the data measurement

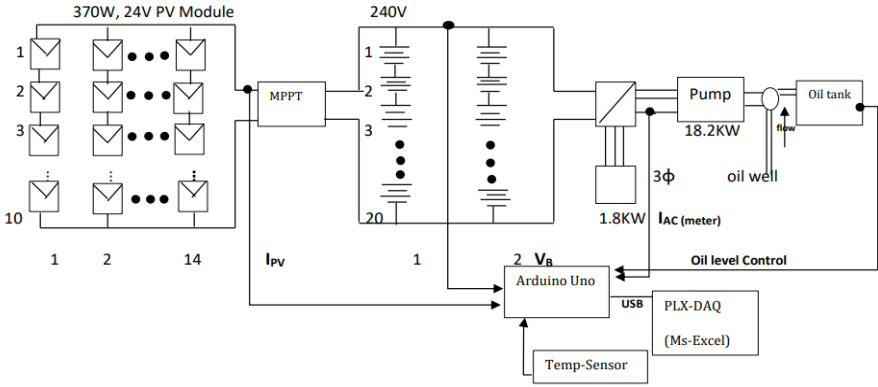


Figure 3:1: Instrumentation Block Diagram

### 3.4 P.L.X. - D.A.Q. and Syntax

PLX-DAQ is an add-on tool of Microsoft Excel that connects any device that supports serial port protocol to Microsoft Excel running on a Windows computer. As seen in figure 2, the PLX-DAQ user interface.

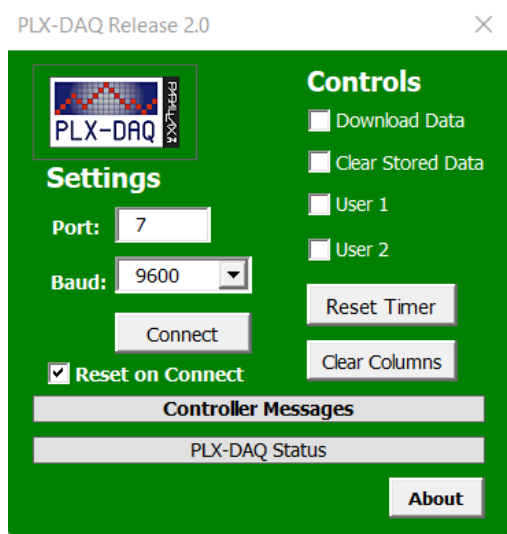


Figure 3:2: PLX DAQ User interface

The PLX DAQ connects to any Arduino device that delivers properly formatted commands for communication and operates with a specific Microsoft Excel Spreadsheet. These instructions may also use variables, functions, and parameters; because the PLX-DAQ and Arduino devices depend on UART serial connection, we employ functions from the serial class, mainly `Serial.print()` and `Serial.println()`.

The command `Serial.println("CLEARDATA")` erases all information from the Excel sheet, including the labels. This command should be the initial command on the sketch, and it cleans out any logged data from previous project. `Serial.println("LABEL,DATE,TIME,")` is the designated labels for the Excel sheet's top row. The most fundamental command in PLX-DAQ is `Serial.print("DATA, DATE, TIME,")`, which is to transfer data from Arduino to Excel and print it excel sheet . When putting data into the rows of Excel sheet, the data should be separated by commas with `Serial.print(",");` denoting a separation between item.

In most circumstances, numerous variables exist in a single Excel spreadsheet row, to enter this variable, the Serial.print() function to used first, then to the next column and signal, we use the Serial.print(","); and the command Serial.println() for the variable.

### 3.4.1 Real-time instrumentation Circuit diagram and material

The circuit diagram in figure 3 below shows a detailed simulation of the system monitoring. Current sensor and voltage sensor are connected to feed from one soure, an LED is connected to the sensor through a 470 ohms resistor in order to measure the current flowing in it. A lighting indicator is use for the oil level montoring control.

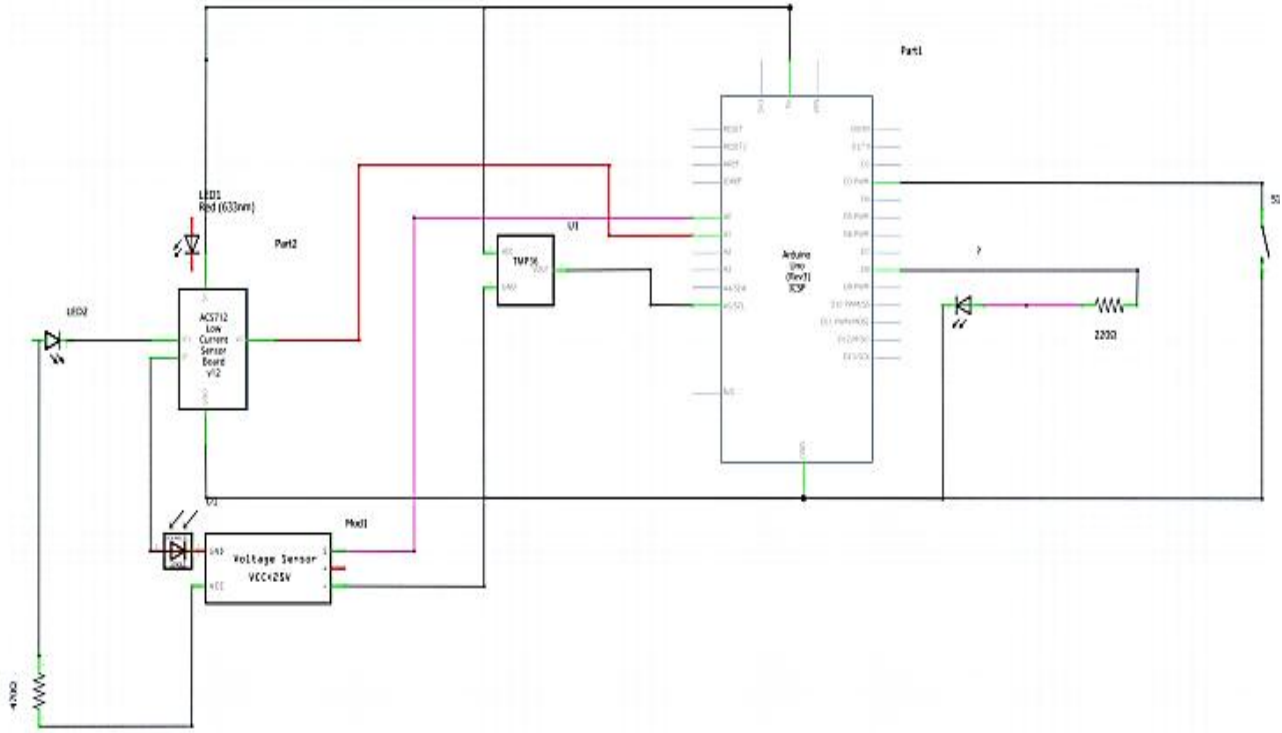


Figure 3:3: Circuit Diagram Schematic

The following hardware used for this implementation

### **Arduino UNO**

This hardware is a microcontroller board with digital and analog pins that are essential for data acquisition. The Arduino UNO with ATmega328 chip microcontroller is use as the membrane for the control.

### **Voltage sensor**

The voltage sensor module measures the voltage from the power supply. The PV output voltage, which ranges between 0 and 24V, is reduced to another voltage ( $V_d$ ), which ranges between 0 and 5V so that Arduino can measure it because the analogue input can only accept voltages up to 5 V. For this circuit, the F031-06 voltage sensor module is use with the following connecting pins shown in figure 4 and the definition [9].



Figure 3:4: Voltage Sensor image

The positive side of the voltage to be measure is connect to VCC. S Pin is connect to an Arduino analogue input, which is the measured output, and GND is connect to the negative of the voltage to be measure, the same electrical point as Arduino ground. The positive pin is disconnect from

any terminal, and the negative terminal is connect to Arduino ground. The Arduino microcontroller's analog-to-digital converter (ADC) generates a digital value ( $V_{out1}$ ) that is encode in 10 bits and has a value range of 0 to 1023. The voltage sensor module has a 5V/1023 analogue voltage resolution and can detect input voltages as low as  $0.00489 \text{ V} \times 5$ . Therefore, the sensor module's voltage range is [0, 25 V]. The equation shown can be use to determine the actual output voltage of a PV panel with the resistor parameters in Figure 3.

$$V = \frac{(R_1+R_2)}{R_2} \times V_{OUT1} \times \frac{5}{1023}$$

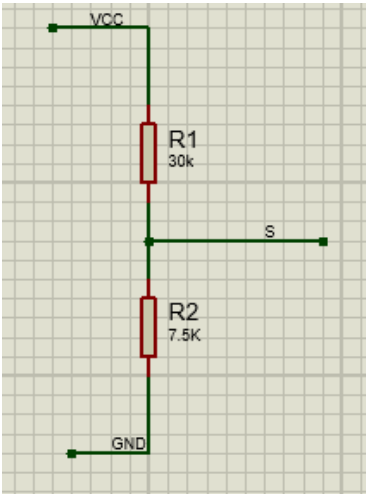


Figure 3:5: Voltage divider embedded in the voltage sensor IC

**Current sensor**

The ACS712 chip uses the Hall Effect to measure DC/AC. For this circuit ACS712ELCTR-05B-T model and datasheet is used shown in figure 7. Figure 6 below shows various models and the output sensitivity of each model.

Part Number	Packing*	T <sub>A</sub> (°C)	Optimized Range, I <sub>p</sub> (A)	Sensitivity, Sens (Typ) (mV/A)
ACS712ELCTR-05B-T	Tape and reel, 3000 pieces/reel	-40 to 85	±5	185
ACS712ELCTR-20A-T	Tape and reel, 3000 pieces/reel	-40 to 85	±20	100
ACS712ELCTR-30A-T	Tape and reel, 3000 pieces/reel	-40 to 85	±30	66

Figure 3:6: ACS712 Model and Output Sensitivity [10]

Sensor sensitivity means that for any model, such as the 5amp model, when the input current increases by 1 amp, the sensor's output voltage increases by about 185 mV [11].

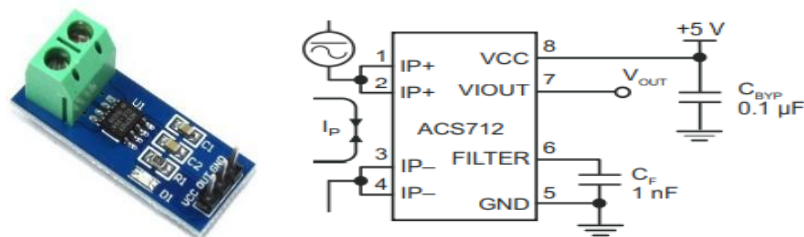


Figure 3:7: Current Sensor and the internal datasheet [11]

VCC is connect to the power supply (5 Volt), GND is connect to the ground, and the OUT is connect to any analog pin in the Arduino.

#### Temperature Sensor TMP36

The TMP36, shown in figure 8, measures temperatures between  $-40^{\circ}\text{C}$  and  $125^{\circ}\text{C}$ . With outputs of 750mV at  $25^{\circ}\text{C}$ , and runs up to  $+125^{\circ}\text{C}$  from a single 2.7 V supply [11]. Pin 1 connects to 5V, pin2 connects to the analog pin, and pin 3 connects to the GND of the Arduino



Figure 3:8: TMP36, Temperature Sensor.

TMP36 analog temperature sensor specifications [11]

Supply voltage	2.7 V to 5.5 V
Quiescent current	50 $\mu$ A
Temperature range	-40°C to + 125°C
Accuracy	$\pm 1^\circ\text{C}$ at +25°C, $\pm 2^\circ\text{C}$ from -40°C to +125°C
Output scale factor	V/°C

Table 3.1: TMP36 Specification

### Float Switch

A float sensor or float switch is implement in the circuit when determining the oil level in an oil tank for a solar pumping system. Because it operates similarly to a switch, it is also known as a magnetic float sensor or float switch. The magnetic float sensor functions as an electromagnetic ON/OFF switch. Making a switching connection allows it to detect the tank's oil level. In this circuit, LED is use as an indicator for the oil level shown in figure 3. Figure 3

shows the float switch connection; one wire is connect to the digital pin and another to the ground.

**Flowchart for the System Monitoring using PLX-DAQ**

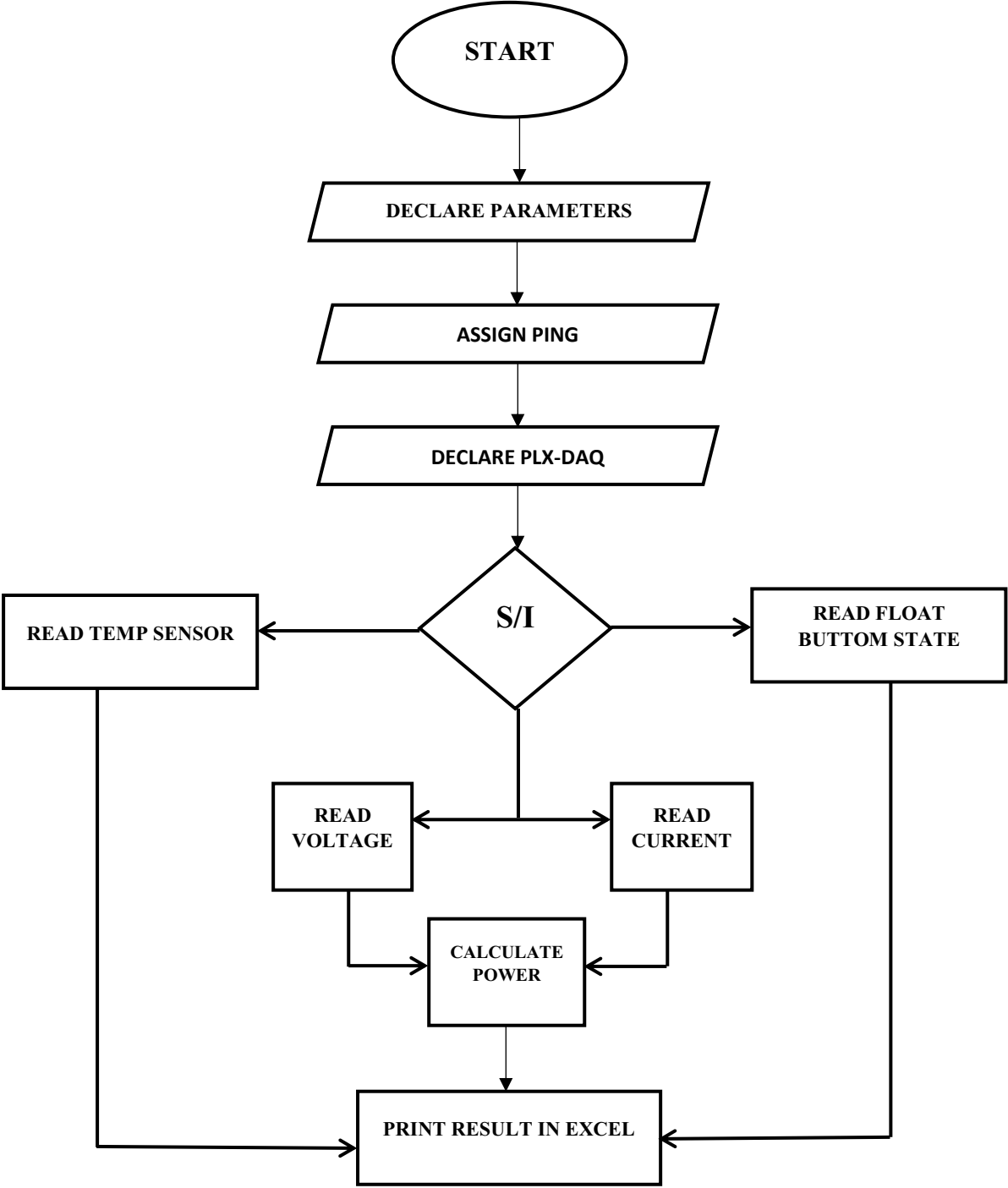


Figure 3:9: Flowchart for the System Monitoring of PLX-DAQ

### 3.5 Results from Plx-Daq

The simulation limitation is that the current sensor is limited to 5A, the voltage sensor is limited to a range  $\ll 25V$  and the temperature sensor measures between  $-40^{\circ}C$  and  $125^{\circ}C$ . For practical demonstration, the results shown below were carry out using a 9V battery, and the temperature sensor was varied under different environmental temperatures. One major limitation for PLXDAQ is that the Float switch outputs read between 1 and 0. `Serial.print(buttonState)` will only give the digital indication of 1 when the oil level is high and 0 when the oil level is low as seen in figure 3.11 .

Figure 3.9 shows the data readings collected in the excel spreadsheet from the Arduino for the practical demonstration. Line because of the introduction the overall monitoring in figure 3.10 shows a spike in the temperature of a hot surface around the environment to test the sensor. The entire data chart is shown in figure 3.13, while the voltage, current and power data logging is shown in figure 3.12.

	A	B	C	D	E	F	G
1	2023-01-21	0.54	Oil level	current (A)	voltage (V)	Power (W)	Temp (c)
2	2023-01-21	12:50:57 PM	1	0.03	8.33	0.22	19.34
3	2023-01-21	12:51:00 PM	1	0.05	8.33	0.44	18.85
4	2023-01-21	12:51:02 PM	1	0.05	8.33	0.44	18.85
5	2023-01-21	12:51:04 PM	1	0.05	8.33	0.44	19.82
6	2023-01-21	12:51:06 PM	0	0.05	8.33	0.44	19.82
7	2023-01-21	12:51:08 PM	0	0.05	8.33	0.44	19.34
8	2023-01-21	12:51:10 PM	0	0.05	8.33	0.44	19.82
9	2023-01-21	12:51:12 PM	0	0.05	8.33	0.44	19.82
10	2023-01-21	12:51:14 PM	0	0.05	8.33	0.44	19.82
11	2023-01-21	12:51:16 PM	1	0.05	8.33	0.44	19.34
12	2023-01-21	12:51:18 PM	1	0.05	8.33	0.44	18.85
13	2023-01-21	12:51:20 PM	1	0.05	8.33	0.44	18.85
14	2023-01-21	12:51:22 PM	1	0.05	8.33	0.44	18.85
15	2023-01-21	12:51:24 PM	1	0.05	8.33	0.44	19.34
16	2023-01-21	12:51:26 PM	1	0.05	8.33	0.44	19.34
17	2023-01-21	12:51:28 PM	1	0.05	8.33	0.44	19.34
18	2023-01-21	12:51:31 PM	1	0.05	8.33	0.44	19.82
19	2023-01-21	12:51:33 PM	0	0.05	8.33	0.44	19.82
20	2023-01-21	12:51:35 PM	0	0.05	8.33	0.44	19.34
21	2023-01-21	12:51:37 PM	0	0.05	8.33	0.44	19.82
22	2023-01-21	12:51:39 PM	1	0.05	8.33	0.44	19.34
23	2023-01-21	12:51:41 PM	1	0.05	8.33	0.44	18.85
24	2023-01-21	12:51:43 PM	1	0.05	8.33	0.44	19.34
25	2023-01-21	12:51:45 PM	1	0.05	8.33	0.44	19.34
26	2023-01-21	12:51:47 PM	1	0.05	8.33	0.44	18.85
27	2023-01-21	12:51:49 PM	1	0.05	8.33	0.44	18.85
28	2023-01-21	12:51:51 PM	1	0.05	8.33	0.44	18.85
29	2023-01-21	12:51:53 PM	1	0.05	8.33	0.44	19.34

Figure 3:10: Data readings in Excel spreadsheet.

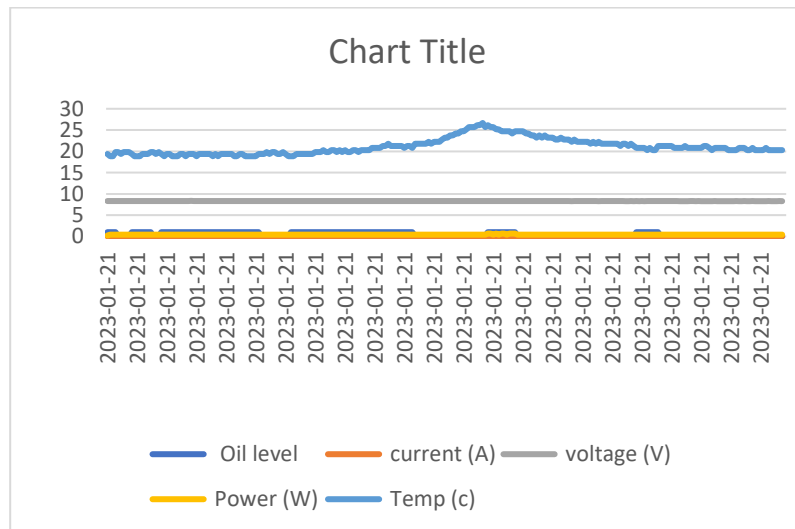


Figure 3:11: Overall data plot in Excel.

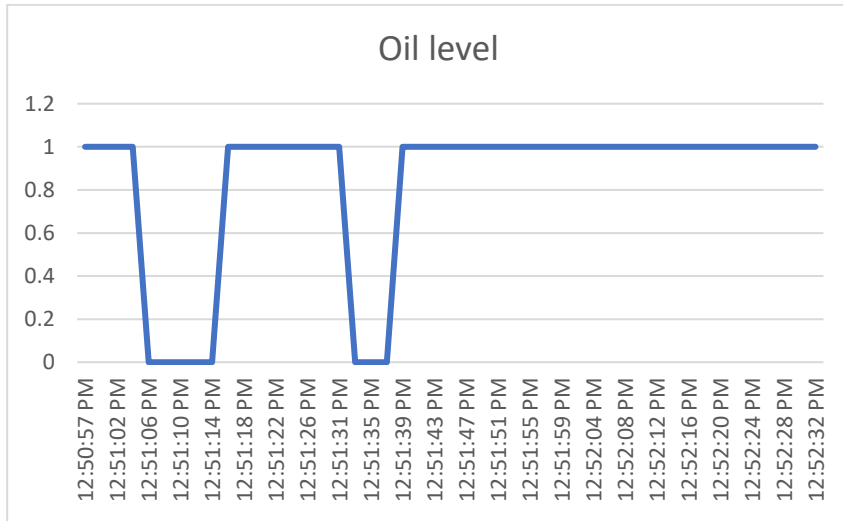


Figure 3:12: Oil level float switch status

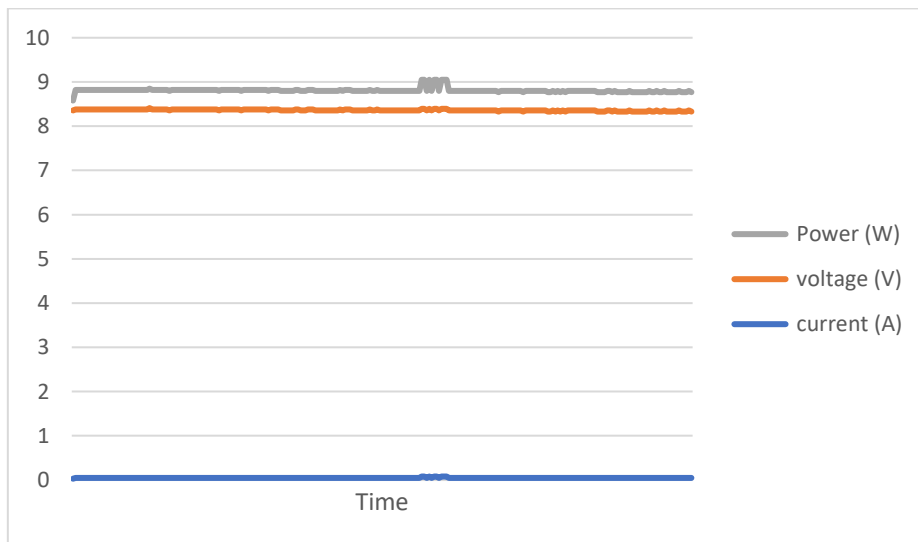


Figure 3:13: Voltage, Current and Power data from a lab test setup

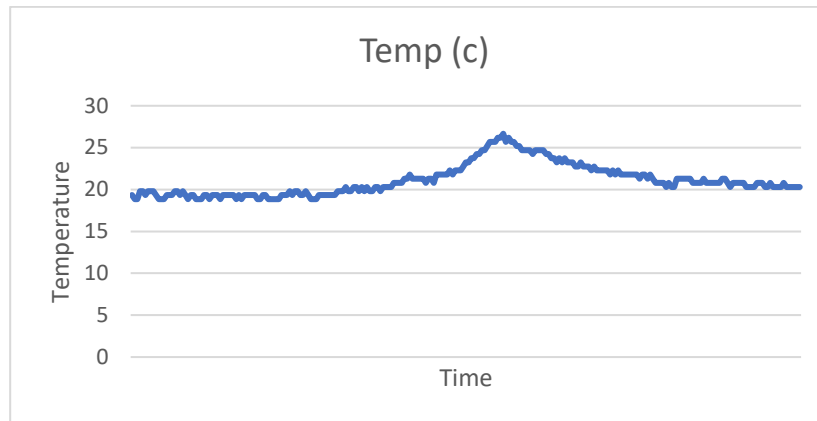


Figure 3:14: Temperature Data Chart

The results above are from a lab test and do not represent the data of an oil well pumping. The system's voltage, current and power data chart dynamics are identical, which shows that once the power source deflects, there will be a change in the entire system's performance. This paper's power source is renewable energy and is subject to environmental change. Monitoring the system is vital for system evaluation, and introducing low-cost data logging will save costs.

### 3.6 Conclusion

To solve the issue of oil spillage from an abandoned oil well, a solar-powered pump was primarily introduced for the oil well remote site. The introduction of renewable energy sources reduces the cost of production, and the system design was done in a previous paper. The introduction of PLX DAQ provides low-cost data logging instrumentation that accurately records system design characteristics in real-time, such as the voltage and current of the PV, AC from the inverter, oil level monitoring, temperature, and relative humidity. This paper

presented a low-cost monitoring system for a remote oil well. Furthermore, this data logger has low maintenance costs, and the saved data are used further for analysis.

### 3.7 Bibliography

- [1] C.O.Okoye and O. Solyali, "Optimal sizing of stand-alone photovoltaic systems in residential buildings", "Energy", vol. 126, pp. 573-584, 2017.
- [2] S. Mekhilef, R. Saidur, and M. Kamalisarvestani, "Effect of dust, humidity and air velocity on efficiency of photovoltaic cells", "Renewable and Sustainable Energy Reviews", vol. 16: 2920-2925, 2012.
- [3] V.V. Tyagi, N.S.A. Rahim, N.A. Rahim, and JAL Selvaraj, "Progress in solar PV technology: Research and achievement", "Renewable and Sustainable Energy Reviews", vol. 20, pp. 443- 461, 2013.
- [4] M. V. Sreenivas Rao and M. Shivakumar, "PLX-DAQ-Based Wireless Battery Monitoring System for Obstacle Avoidance Robot," *Control Instrumentation Systems*, pp. 133–140, Aug. 2019, doi: 10.1007/978-981-13-9419-5\_12.
- [5] B. Maharmi, B. Widyastomo, and F. Palaha, "Water Flow Measurement-Based Data Acquisition Using Arduino Microcontroller and PLX-DAQ Software," *Jurnal Ilmiah Teknik Elektro Komputer dan Informatika*, vol. 8, no. 1, pp. 107–118, Apr. 2022, doi: 10.26555/jiteki.v8i1.23637.
- [6] M. Fuentes, M. Vivar, J.M. Burgos, J. Aguilera, and J.A. Vacas, "Design of an accurate, low-cost autonomous data logger for PV system monitoring using Arduino™ that complies with IEC standards", "Solar Energy Materials & Solar Cells", vol. 130, pp. 529-543, 2014.
- [7] N. Sugiarta, I. M. Sugina, I. D. G. A. T. Putra, M. A. Indraswara, and L. I. D. Suryani, "Development of an Arduino-based Data Acquisition Device for Monitoring Solar PV System Parameters," *Proceedings of the International Conference on Science and Technology (ICST 2018)*, 2018, doi: 10.2991/icst-18.2018.201.

- [8] O. Chidolue and T. Iqbal, "Solar Powered Pump for a Remote Oil Well in Nigeria," *Memorial University Research Repository*, Nov. 15, 2022. <https://research.library.mun.ca/15783/> (accessed Jan. 20, 2023).
- [9] ArduinoVoltageSensor [http://www.ekt2.com/pdf/412\\_ARDUINO\\_SENSOR\\_VOLTAGE\\_DETECTOR.pdf](http://www.ekt2.com/pdf/412_ARDUINO_SENSOR_VOLTAGE_DETECTOR.pdf), accessed January 20, 2023.
- [10] Fully Integrated, Hall Effect-Based Linear Current Sensor IC with 2.1 kVRMS Isolation and a Low-Resistance Current Conductor, <https://www.allegromicro.com/en/search?q=acs712%20datasheet>, accessed January 20, 2023.
- [11] alldatasheet.com, "TMP36 Datasheet(PDF) - Analog Devices," *Alldatasheet*.<https://www.alldatasheet.com/datasheet-pdf/pdf/49108/AD/TMP36.html> (accessed Jan. 20, 2023).

## Chapter 4

### **REAL-TIME MONITORING AND DATA ACQUISITION USING LORA FOR A REMOTE SOLAR POWERED OIL WELL.**

#### ***Preface:***

*A version of this manuscript is in review under **Journal of International Journal of Applied Power Engineering (IJAPE)**. I am the primary author, and I carried out most of the research work, performed the literature reviews, carried out the system design, modeling, and analysis of the results. I also prepared the first draft of the manuscript and subsequently revised the final manuscript based on the feedback from the co-author and the peer review process. The Co-author, Dr. M. Tariq Iqbal, supervised the research, acquired, and made available the research funding, provided the research guide, reviewed and corrected the manuscript, and contributed research ideas in the actualization of the manuscript.*

#### ***Abstract***

Real-time monitoring is essential for solar-powered systems as they can be affected by sudden environmental changes, which may occur unpredictably, especially in isolated regions without internet connectivity. This study proposes a wireless communication-based approach that allows for data acquisition and system monitoring of the entire solar system, which is particularly important in remote areas. The proposed instrumentation method offers an affordable solution for monitoring the battery voltage, photovoltaic (PV) current, the converter's alternating current (AC), and oil well management. These measurements rely solely on solar irradiation, which can significantly impact the overall performance of the solar-powered system. A wireless communication tool for a long range called LoRa was used, the

TTGO LoRa32 SX1276 OLED as the sender node and Heltec LoRa esp 32 as the transmitter node. These IC's are ESP32 development boards with an integrated LoRa chip and an SSD1306 flash memory.

#### **4.1 Introduction**

Real-time monitoring is essential for solar-powered systems as they can be affected by sudden environmental changes, which may occur unpredictably, especially in isolated regions. This study proposes a wireless communication-based approach that allows for data acquisition and system monitoring of the entire solar system of a remote oil well. The proposed instrumentation method offers an affordable solution for monitoring the battery voltage, photovoltaic (P.V) current, the converter's alternating current (A.C), and oil well management. A wireless communication tool for a long-range called LoRa is used, with the TTGO LoRa32 SX1276 OLED as the sender node and Heltec LoRa esp 32 as the transmitter node. These I.C.s are ESP32 development boards with an integrated LoRa chip and an SSD1306 flash memory. System design and some test results are included in this chapter.

In areas lacking connectivity or internet access, transmitting sensor data from one location to another can pose challenges. In such situations, wireless sensor monitoring systems are often employ to transfer data from low network coverage areas to sites with internet access. This process involves utilizing a LoRa module transmitter to receive sensor data in the low network coverage area. Subsequently, the data is transmit from the LoRa sender node to a receiver node to establish a gateway connection to the cloud. As a result, the data becomes accessible from any location, facilitating real-time updates of cloud data. The system typically comprises a sender node, receiver node, and display unit for data acquisition [1, 2].

Utilizing a LoRa module within a wireless sensor network enables remote system monitoring in remote locations, such as rural areas, forests, farms, and national roads, where network connectivity is limited. By connecting LoRa modules with sensors, this network facilitates remote data access from diverse regions. Furthermore, the network's low power consumption makes it well suited for security monitoring and surveillance applications. A wireless network using LoRa technology for long-range data transmission for monitoring system comprises nodes and a gateway. LoRa operates on low power, making it suitable for battery-operated applications that require end-to-end communication. LoRa can detect specific sensor data type, transmit, and receive it over far distances, even without internet access, while requiring very little power [3]. In a literature survey conducted in [4], the authors primarily focus on Long Range Wide Area Network (LoRaWAN) and its application in Water Grid. The LoRaWAN technology is made up of relay node discovery, LoRa modulation, layer formation, LoRaWAN protocol clustering, spreading factor assignment, network joining, data transmission, flow table setup and protocol requirements and validation. The developed algorithm demonstrates precision in calculating the rate of error of the packet and single-hop networks energy consumption. However, a limitation or research gap identified in this study is the lack of evaluation for the number of nodes in each relay node [4]. The system uses Ra-02 LoRa modules to send data from the sender node to the receiver node. The sender node receives and sends the sensor data to the receiver node using LoRa and ESP8266 microcontroller. In addition, solar panels driven by low power consumption can be used for power supply. The received data is then updated in a database using the Wi-Fi network. LoRa technology, specifically LoRaWAN, is a technology utilized in Low Power Wide Area Networks (LPWAN), as mentioned in [5], this LoRa technology is a proprietary development of Semtech Technology [6].

LoRa offers an optimized combination of long-range communication, secure data transmission and low power consumption by incorporating the spread spectrum modulation technique derived from Chirp Spread Spectrum and integrated Forward Error Correction. The LoRa Alliance developed LoRaWAN [6, 7] as an open standard with the network, MAC, and application layers. These combined technologies enable wide-area communication, low-power consumption, and gateways in Wireless Sensor Networks, catering to low-latency, low-bandwidth Internet of Things (IoT) applications. The LoRa wide area network protocol, also known as LoRa, offers interoperability among LPWAN networks and delivers additional advantages, including easy installation, cost-effectiveness, flexibility, scalability, bi-directionality, security, and encryption. LPWAN technologies have the potential to support a massive number of devices in the future Internet of Things. Specifically, LoRaWAN technology is optimized for sensor-based IoT applications where only small amounts of data must be transmitted over long distances, resulting in efficient battery life. Designed within the LPWAN space, LoRaWAN prioritizes range, battery life, and cost to cater to the requirements of such IoT applications [8, 9].

#### 4.1.1 Lora Sender

The flowchart shown in Figure 4.1 illustrates the systematic process utilized to initialize the setup, collect sensor information, and transmit the data as packets to the receiver node. The depicted sequence of events in the flowchart starts with initializing the LoRa receiver module and the hardware system, followed by sensor data acquisition. Subsequently, the data is transmitted to the receiver node, and the packets' status is displayed.

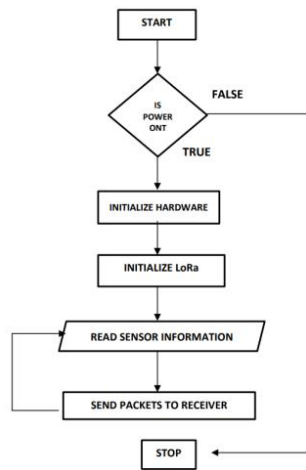


Figure 4:1: LoRa Sender Node FlowChart

#### 4.1.2 Lora Receiver

The Receiver node executes a similar sequence of events as the sender node, except for the absence of transmission of sensor data, which is exclusive to the sender, as shown in Figure 4:2. The transmitter LoRa node sends the data in the form of packets and is receive by the receiver LoRa module. The OLED display shows the status of the packet received. The following flowchart presents the system of methods employed in the receiver node.

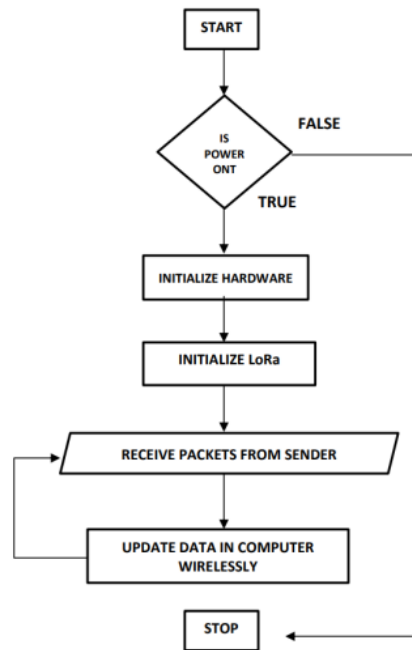


Figure 4:2: Lora Receiver Node Flowchart

## 4.2 Wireless Communications

Cellular networks are extensively utilized because they provide high-speed data coverage. However, for IoT applications, high-speed data is not always essential. Devices that rely on cellular networks often suffer from short battery life and encounter coverage gaps. In contrast, ZigBee mesh networks are popular in home automation because of their reliable performance over short to medium distances. However, they are not suitable for long distances of a few kilometres. Bluetooth/BLE data rates are moderate, but the range is severely restricted.

The IEEE802.11 WLAN standard is one of the most prevalent wireless methodologies utilized today, primarily due to its high data rate and bandwidth capabilities. However, it has limitations such as limited range and high battery consumption. Wi-Fi devices often have short battery life and must be close to the Wi-Fi access point for effective communication. Additionally, operating frequencies of 2.4 and 5 GHz of Wi-Fi signals make them less effective at passing

through obstacles. When overcoming these limitations, LoRaWAN technology is a promising solution for IoT-driven applications in various fields [10].

### **4.3 Advancement of Lora Technology**

In the study [11], the paper discussed the implementation of a LoRa network server on the OpenStack platform. They successfully updated the operations of the LoRa network server to achieve service flexibility and scalability by leveraging the system services provided by OpenStack. They created an experimental setup to validate their approach utilizing commercially available LoRa hardware, an open-source terminal, a gateway, and OpenStack software. To address the challenge of transmitting large amounts of data, the authors utilized Wi-Fi service to overcome the limitation of low data rates in LoRa technology. By combining these two technologies, they developed a multi-interface communication module that could meet the requirements of long-range communication and low-power operation with LoRa, while also enabling the transmission of large data volumes using wireless LAN (Wi-Fi).

The design principles of LoRa technology encompass various aspects such as modulation, receiver sensitivity, and spreading factor. The Spreading Factor quantifies the relationship between the chips and bits, a crucial parameter in LoRa modulation [12]. LoRa technology employs CSS modulation, allowing flexible long-distance communication while minimizing power consumption by utilizing different spreading factors (S.F). The S.F value can be adjusted from 7 to 12, resulting in LoRaWAN transmitting rates ranging from 0.3 to 27 kbps. A higher S.F value leads to increased communication range and prolongs the duration of data packet transmission in the air [12, 13].

In the context of large-scale implementation, LoRa, a wireless sensor network (WSN), is highly valuable due to its utilization of both network and node characteristics. LoRa sensor networks

are employed by utility companies to connect end-user devices to their network, facilitating streamlined administration. Similarly, in urban areas, LoRa networks are used by cities to pioneer "smart" concepts aimed at improving the efficiency of resource and service administration. Additional applications of LoRa networks include an automated reading of water meters for water companies, eliminating the need for on-site human intervention, and citywide intelligent parking solutions. In traditional rural environments with limited resources, LoRa sensors can also be applied to intelligent agriculture applications [14]

In a study conducted by [15], commercially available equipment was used to investigate the distance coverage of LoRaWAN technology in two different scenarios. The data was collected by deploying a node on land and another node on water, and both reported data to a base station. Based on the collected data, the authors calculated the communication range of LoRaWAN to be 15 km on land and 30 km on water.

The LoRa wireless networks performance evaluation was presented in [16], the assessment analyzes the impact of bitrate, Time on Air (ToA), and S.F. on performance levels. The findings reveal that increasing the S.F. parameter results in a corresponding increase in ToA. However, a significant reduction in ToA is observed with increased communication channel bandwidth. This Chapter [17] presents results on data compression in wireless sensor nodes utilizing LoRa technology for data transmission. Additionally, a comparison of energy consumption is conducted with other commonly used data communication protocols in Wireless Sensor Networks (WSN), such as ZigBee, to highlight the advantages of LoRa. While [18] proposed a dual-key scheme to enhance the security of LoRa. Although the proposed plan was deemed adequate, it was found to have increased computing requirements, resulting in higher power consumption and system costs. This challenges meeting the demand for low power, long-range,

high-data transmission anticipated with IoT commercialization. Specifically, the data transmission rate in the proposed scheme was observed to be low.

This paper will update the received data in a computer display instead of using a Wi-Fi module. LoRa technology will send and transmit the analyzed P.V. system performance data collected locally in PLX DAQ for further analysis in [19]. A low-cost monitoring system for a solar oil pumping system is proposed and will be helpful in small remote stripper oil wells.

**4.4 Methodology**

The instrumentation block diagram of a remote solar oil well is depicted in Figure 4.3, and this real-time monitoring system can measure the energy flow and oil level and monitor the energy by measuring various parameters such as battery voltage, A.C. current from the inverter, and power. The data in [19] measurements are recorded in a plug-in called PLX-DAQ (Parallax Data Acquisition); this chapter aims to transmit the data wirelessly using LoRa by using Heltec LoRa 32 device and TTGO LoRa32.

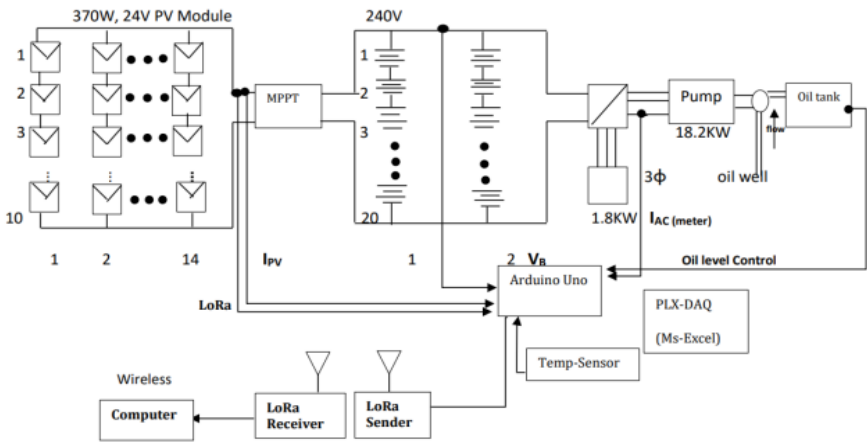


Figure 4.3: Instrumentation Block Diagram of the Entire Monitoring System

#### 4.4.1 Instrumentation Circuit Design and Calibration

The circuit includes a temperature sensor, a current sensor and a voltage sensor that are connected to a common power source. Additionally, a level indicator is employed for oil level monitoring. The following hardware is used for wireless data transmission.

##### I. Temperature Sensor -DHT11

This sensor ensures exceptional reliability and accuracy; it reads the digital signal output, which is then linked to a high-performance 8-bit microcontroller. The sensor incorporates a resistive-type humidity measurement component and a Negative Temperature Coefficient (NTC) measuring component, resulting in outstanding quality, rapid response, immunity to interference, and cost-effectiveness. It operates within a temperature range of 0 to 50°C and a humidity range of 20% to 90%, offering precise measurements with a precision of 1°C for temperature and 1% for humidity. The DHT11 sensor is available in two pin layouts: a four-pin option and a three-pin option. In this thesis, the three-pin configuration is utilized, where Vcc serves as the power supply, Ground functions as the circuit ground, and Data serves as the serial data output for temperature and humidity readings. The sensor operates within a voltage range of 3 - 5.5 V, and a 10kΩ pull-up resistor is employed to connect the output pin to the microcontroller's Vcc. The power supply is denoted as Vcc, the circuit ground as ground, and the serial data output for reading temperature as Data. For this work, the data pin of the sensor will be connected to GPIO 33 of the Heltec Lora 32 microcontroller, shown in Figure 4.

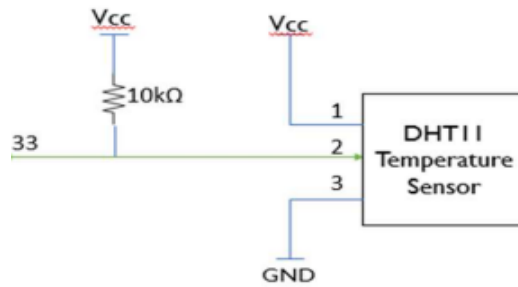


Figure 4:4: Temperature Sensor Circuit Connection.

## II. Voltage Sensor Connection

The voltage measurement of this sensor is based on the voltage divider principle, which utilizes a series connection of 7.5 k and 30 k resistors to create a 5-to-1 voltage divider for accurate measurement shown in Figure 6. The sensor operates within a voltage range of 3.3 - 5.0 V and can monitor the voltage in the 0 - 25 V DC range using a 12-bit ADC. It is worth noting that the ESP32 microcontroller requires a 3.3 V input voltage for proper functioning. To connect the voltage sensor to the ESP32 microcontroller, pin S of the sensor is linked to analog pin 32 of the ESP32, while pin - is connected to the GND pin, as shown in Figure 5. The F031-06 voltage sensor module is used. The voltage sensor module has a resolution of 3.3 V/4095 analog voltages, allowing it to detect input voltages as low as 0.0008058 V multiplied by 5. With the resistor specifications in the circuit diagram in Figure 6, the provided equation can be used to calculate the actual output voltage of a photovoltaic (P.V.) panel.

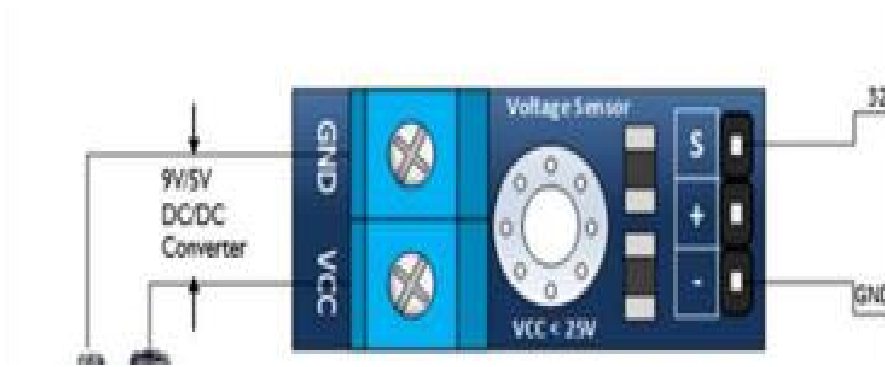


Figure 4:5: Voltage Sensor Connecting Circuit

$V = \frac{(R_1+R_2)}{R_2} \times V_{OUT1} \times \frac{3.3}{4095}$ . The equation is the voltage divider principle used for the esp32 connection.

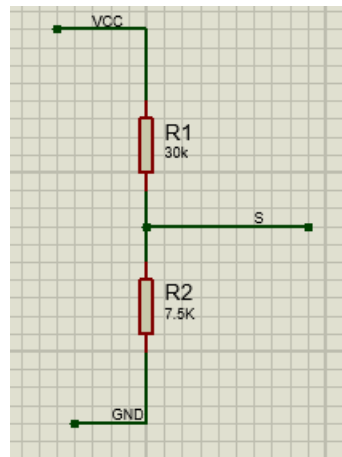


Figure 4:6: Voltage Divider rule embedded in the IC

### III. Current Sensor

The ACS712 chip measures DC/AC by the Hall Effect. Figure 7 shows the ACS712ELCTR-05B-T model and datasheet utilized for this circuit.

Part Number	Packing*	T <sub>A</sub> (°C)	Optimized Range, I <sub>p</sub> (A)	Sensitivity, Sens (Typ) (mV/A)
ACS712ELCTR-05B-T	Tape and reel, 3000 pieces/reel	-40 to 85	±5	185
ACS712ELCTR-20A-T	Tape and reel, 3000 pieces/reel	-40 to 85	±20	100
ACS712ELCTR-30A-T	Tape and reel, 3000 pieces/reel	-40 to 85	±30	66

Figure 4:7: ACS712 and Model Sensitivity [10]

The current is determined by measuring the voltage generated by a fully integrated, low-cost, high-precision sensor. This sensor utilizes a non-invasive approach to detect current by sensing the magnetic field generated around the wire. It employs a low-resistance current conductor and can measure both D.C. and A.C. currents. The ACS712 Hall-Effect sensor is available in three sizes: 5A, 20A, and 30A. When no current is detected, it outputs a voltage of 2.5 V DC. The sensor's sensitivity varies depending on the module size, ranging from 66 mV/A for the 5A module, 100 mV/A for the 20A module, and 185 mV/A for the 30A module in Figure 7. In Figure 4.8, a voltage divider is used to reduce the voltage from 5V to 3.3V since the Esp32 pins are powered by 3.3V.

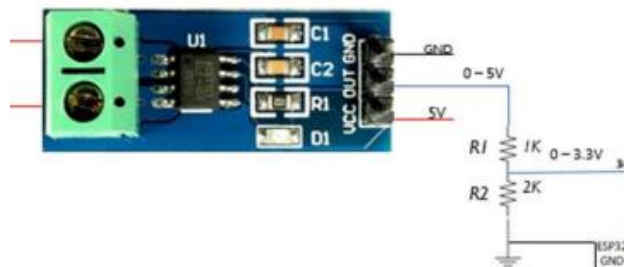


Figure 4:8: Current Sensor Connecting Circuit

## **Float switch**

A float sensor is integrated to determine the oil level in an oil tank in a solar pumping system. An electromagnetic ON/OFF switch, like a magnetic sensor, detects the tank's oil level by establishing a switching connection. In the circuit connection, one wire is connected to the ground and the other is connected to any digital pin. It is used to measure the level of the oil tank.

### 4.4.2 LoRa code and syntax explanation for the system instrumentation

#### LoRa Sender

When facilitating the configuration of LoRa, including the library that facilitates the communication between the TTGO LoRa 32 and the LoRa transceiver module is necessary. Additionally, it is imperative to specify the specific pins employed by the LoRa Sender module. Within the `setup()` function, it becomes essential to carry out a manual software reset of the OLED by utilizing the RST pin. This reset entails declaring the RST pin as an output, setting it to a LOW state, and reverting it to a HIGH state. Initializing the user interface (U.I.) will also initialize the display. To designate the LoRa node, the phrase "LORA SENDER" should be displayed on the screen for identification. In order to identify and establish the necessary connections for the LoRa chip, the LoRa transceiver module utilizes the SPI pins and must be defined. Subsequently, initialize the LoRa transceiver module by invoking the `begin()` method on the LoRa object and specifying the desired frequency as a parameter. Upon successful initialization of the display, a message indicating success will be exhibited on the OLED display. In the `loop()` function, the transmission of packets will occur. The `beginPacket()` method is employed to commence a packet, while the `print()` method is utilized to incorporate data into the packet. Finally, the `endPacket()` method is used to finalize the packet.

#### LoRa Receiver

The syntax for the receiver code is similar to the sender. In order to streamline the configuration process of LoRa, it is essential to integrate the appropriate library that facilitates seamless communication between the Heltec ESP32 and the LoRa transceiver module. Furthermore, it is crucial to explicitly define the pins employed by the LoRa Receiver module. Within the `setup()` function, the execution of a manual software reset for the OLED becomes necessary, wherein the RST pin is utilized. This reset procedure involves declaring the RST pin as an output, setting it to a LOW state, and restoring it to a HIGH state. Initialization of the user interface (U.I.) will concurrently initialize the display. To identify the LoRa receiver node, the designation "LORA RECEIVER" should be employed. In the `loop()` function, the transmission of packets received will be parsed. The `int packetSize = LoRa.parsePacket();` is to receive a packet from the sender module, while the `while (LoRa.available()) {` is to read the packet.

#### **4.5 Results**

In the simulation, the ACS712 sensor is limited to 5A maximum current, the F031-06 sensor is limited to a range of 25V maximum voltage, and the DHT 11 sensor is limited to a temperature range of -40°C to 125°C. The results presented below were obtained using a 9V non-rechargeable alkaline battery and changing the oil level for practical demonstration, the circuit diagram and the sender node is seen in Figure 4.9. In Figure 4.10, the receiver node shows just the temperature data and the RSSI, the receiver node used is a Heltec esp32 LoRa. In Figure 4.11, the results were displayed on PuTTY and Figure 4.12 shows that the oil level was high from counter 71, RSSI 32. For further data analysis, PLX-DAQ was used in the previous study [8] to evaluate the data further.

Serial.println(currentButtonState); currentCounter=LoRa.readStringUntil('|'); will only return 1 when the oil level is high and 0 when the oil level is low, as shown in Figure 4.11. The above results are from a lab test and do not represent data from an oil well pumping.

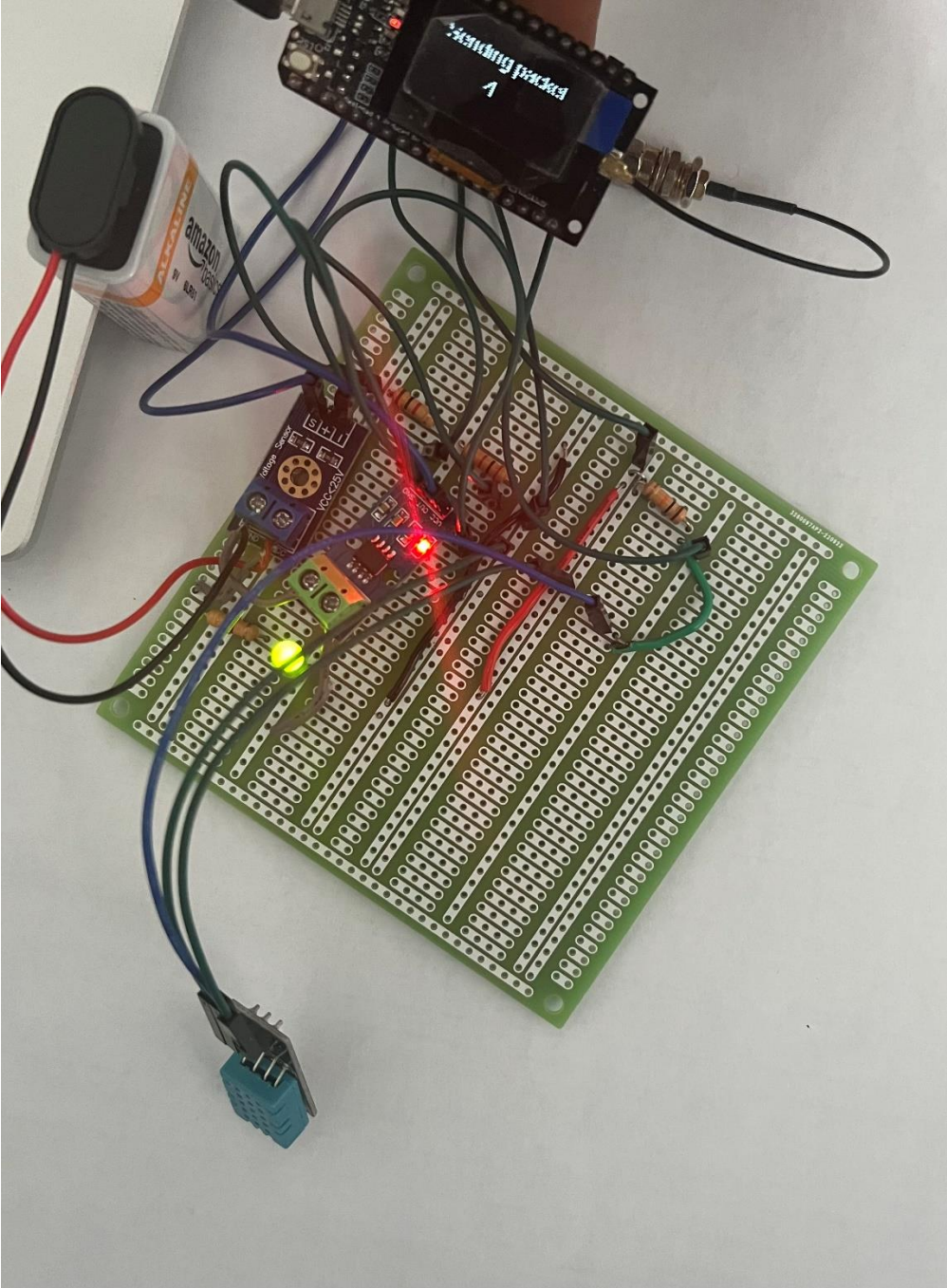


Figure 4:9: Implemented Circuit with Sender Node



Figure 4:10: Receiver Node

```
ets Jun  8 2016 00:22:57

rst:0x1 (POWERON_RESET),boot:0x17 (SPI_FAST_FLASH_BOOT)
configsip: 0, SPIWP:0xee
clk_drv:0x00,q_drv:0x00,d_drv:0x00,cs0_drv:0x00,hd_drv:0x00,wp_drv:0x00
mode:DIO, clock div:1
load:0x3fff0018,len:4
load:0x3fff001c,len:1044
load:0x40078000,len:10124
load:0x40080400,len:5856
entry 0x400806a8
LoRa Receiver
LoRa Initial OK!
Received packet. Temp:26.70
Voltage (V):7.85
current (A):0.45
Power (W):3.55
OilLevel:0
Counter:36
  with RSSI -34
Received packet. Temp:26.70
Voltage (V):7.83
current (A):0.45
Power (W):3.55
OilLevel:0
Counter:37
  with RSSI -33
Received packet. Temp:26.70
Voltage (V):7.81
current (A):0.45
```

Figure 4:11: Data Transmitted wirelessly to PuTTY

```
Received packet. Temp:26.70
Voltage (V):7.80
current(A):0.45
Power(W):3.52
OilLevel:0
Counter:70
  with RSSI -33
Received packet. Temp:26.70
Voltage (V):7.81
current(A):0.46
Power(W):3.57
OilLevel:1
Counter:71
  with RSSI -32
Received packet. Temp:26.70
Voltage (V):7.79
current(A):0.45
Power(W):3.52
OilLevel:1
Counter:72
  with RSSI -31
Received packet. Temp:26.70
Voltage (V):7.80
current(A):0.46
Power(W):3.55
OilLevel:1
Counter:73
  with RSSI -30
Received packet. Temp:26.70
Voltage (V):7.78
current(A):0.46
Power(W):3.56
OilLevel:0
Counter:74
  with RSSI -42
Received packet. Temp:26.70
Voltage (V):7.80
current(A):0.46
Power(W):3.58
```

Figure 4:12: Data indicating that the Oil Level is high

#### 4.6 Conclusion

To tackle the problem of oil spillage from an abandoned oil well, a solar-powered pump was initially installed at the remote location of the well. Using renewable energy sources reduced production costs, and the system design was documented in a prior publication. LoRa wireless communication introduced affordable data logging instruments that accurately captured real-

time information about the system design characteristics, such as P.V. voltage and current, A.C. from the inverter, oil level monitoring, temperature, and relative humidity. This research presents a cost-effective wireless monitoring system for remote oil wells that is also easy to maintain, and the collected data can be utilized for further analysis. This system is particularly suitable for areas without internet connectivity.

#### **4.7 Bibliography**

- [1] K. P. Kamble, "LoRa Communication based Wireless Sensor Monitoring system," 2022 International Conference on Sustainable Computing and Data Communication Systems (ICSCDS), Erode, India, 2022, pp. 1127-1131, doi: 10.1109/ICSCDS53736.2022.9760796.
- [2] Q. Zhou, K. Zheng, L. Hou, J. Xing and R. Xu, "Design and Implementation of Open LoRa for IoT," in IEEE Access, vol. 7, pp. 100649-100657, 2019, doi: 10.1109/ACCESS.2019.2930243.
- [3] R. Kini, A. Biradar, P. Malusare, A. Karelia, and M. Kumar, "LORA BASED DATA ACQUISITION SYSTEM," [www.irjet.net](http://www.irjet.net), Apr. 22, 2022. <https://www.irjet.net/archives/V9/i4/IRJET-V9I4456.pdf>.
- [4] I. Cheikh, R. Aouami, E. Sabir, M. Sadik and S. Roy, "MultiLayered Energy Efficiency in LoRa-WAN Networks: A Tutorial," in IEEE Access, vol. 10, pp. 9198-9231, 2022, doi: 10.1109/ACCESS.2021.3140107.
- [5] IETF RFC837" Low-Power Wide Area Network (LPWAN) Overview" [Online] Available: <https://tools.ietf.org/html/rfc8376>
- [6] A. Siddique, "A Review On Intelligent Agriculture Service Platform With Lora Based Wireless Sensor Network," International Research Journal of Engineering and Technology (IRJET), vol. 06, no. 02, pp. 2539–2542, Feb. 2019.
- [7] Sornin N. (Semtech), Yegin A. (Actility), et all. "LoRaWAN™ Specification," V1.1 Oct. 2017. [Online]. Available: <https://loraalliance.org/resource-hub/lorawantm-specification-v11>

- [8] A. J. Wixted, P. Kinnaird, H. Larijani, A. Tait, A. Ahmadinia, and N. Strachan, "Evaluation of LoRa and LoRaWAN for wireless sensor networks," in Proc. IEEE Sensors, Oct./Nov. 2016, pp. 1–3.
- [9] J. Haxhibeqiri, I. Moerman, and J. Hoebeke, "Low overhead scheduling of LoRa transmissions for improved scalability," IEEE Internet Things J., vol. 6, no. 2, pp. 3097–3109, Apr. 2019.
- [10] Z. Li, J. Wang, R. Higgs, L. Zhou, and W. Yuan, "Design of an intelligent management system for agricultural greenhouses based on the internet of things," in Computational Science and Engineering (CSE) and Embedded and Ubiquitous Computing (EUC), 2017 IEEE International Conference on, vol. 2. IEEE, 2017, pp. 154–160.
- [11] J. So, D. Kim, H. Kim, H. Lee and S. Park, "LoRaCloud: LoRa platform on OpenStack," 2016 IEEE NetSoft Conference and Workshops (NetSoft), Seoul, Korea (South), 2016, pp. 431-434, doi: 10.1109/NETSOFT.2016.7502471.
- [12] Semtech, SX1272/3/6/7/8: LoRa Modem Designer's Guide. 2013. [Online]. Available: [https://www.semtech.com/images/datasheet/LoraDesignGuide\\_STD.pdf](https://www.semtech.com/images/datasheet/LoraDesignGuide_STD.pdf)
- [13] Sornin N. (Semtech), Yegin A. (Actility), et al. "LoRaWAN™ Specification," V1.1 Oct. 2017. [Online]. Available: <https://lora-alliance.org/lorawan-coverage/>
- [14] D. I. Sacaleanu, I. P. Manciu and L. A. Perisoara, "Performance Analysis of LoRa Technology in Wireless Sensor Networks," 2019 10th IFIP International Conference on New Technologies, Mobility and Security (NTMS), Canary Islands, Spain, 2019, pp. 1-5, doi: 10.1109/NTMS.2019.8763774.
- [15] J. Petajajarvi, K. Mikhaylov, A. Roivainen, T. Hanninen and M. Pettissalo, "On the coverage of LPWANs: range evaluation and channel attenuation model for LoRa technology," 2015 14th International Conference on ITS Telecommunications (ITST), Copenhagen, Denmark, 2015, pp. 55-59, doi: 10.1109/ITST.2015.7377400.
- [16] A. Lavric and V. Popa, "A LoRaWAN: Long range wide area networks study," 2017 International Conference on Electromechanical and Power Systems (SIELMEN), Iasi, Romania, 2017, pp. 417-420, doi: 10.1109/SIELMEN.2017.8123360.

[17]D.I. Sacaleanu, R. Popescu, , I. Manciu, L.A. Perisoara. "Data Compression in Wireless Sensor Nodes wirh LoRa" 10th Electronics, Computers and Artificial Intelligence International Conference (ECAI 2018), Iasi, Romania, June 28-30, 2018.

[18] J. Kim and J. Song, "A Dual Key-Based Activation Scheme for Secure LoRaWAN," *Wireless Communications and Mobile Computing*, vol. 2017, p. e6590713, Nov. 2017, doi: <https://doi.org/10.1155/2017/6590713>.

[19] O. Chidolue and T. Iqbal, "System Monitoring and Data logging using PLX-DAQ for Solar-Powered Oil Well Pumping," 2023 IEEE 13th Annual Computing and Communication Workshop and Conference (CCWC), Las Vegas, NV, USA, 2023, pp. 0690-0694, doi: 10.1109/CCWC57344.2023.10099099.

## Chapter 5

### CONCLUSION AND FUTURE WORK

#### 5.1 Conclusion

The impact of an abandoned well with a low production rate on the environment is severe. To mitigate this issue, a cost-effective alternative technology, namely the solar-powered pump, presents an effective solution for oil companies, considering the expensive nature of minimizing the impact caused by pumping the remaining oil. In this context, a comprehensive system sizing approach was proposed for Olobiri oil well 17.

The sizing process involved utilizing PVsyst to recommend the appropriate pump size. The software's performance was evaluated by simulating the oil depth to align with the site's specifications. The results showed that for a 5-hour running time, the system efficiency was 11.4%, and the pump efficiency was 37.9%. Conversely, during continuous flow, the system efficiency was 5%, and the pump efficiency was 11%. The PV setup was properly sized in HOMERpro, considering the overall load of the power system. Based on PVsyst's suggestions, the software recommended a 50kW PV unit and 54.9kW for the batteries, with exact size specifications. Notably, the system's efficiency was found to be higher when operating for 5 hours. For the evaluation of condition A (5 hours running time), a 1.4kW Grundfos Solflex DC pump with a brushless DC motor was used, while for condition B (non-stop running time), a 328W Lorentz DC pump with a brushless DC motor was employed. The results indicated that the system's efficiency was better suited for the location when running for five hours (condition A). The system setup comprised a 22.3kW converter, 40 (970Ah, 12V) batteries, and a 50kW 370W 24V solar panel.

To further mitigate the problem of oil spillage from abandoned oil wells in remote areas, the addition of PLX DAQ facilitated low-cost data logging, recording real-time system design characteristics such as PV voltage and current, AC from the inverter, oil level monitoring, temperature, and relative humidity. The resulting monitoring system is both cost-effective and easy to maintain, with the collected data utilized for further analysis. This system is particularly suitable for areas lacking internet connectivity. The simulation presented certain limitations, such as the maximum current for the ACS712 sensor being 5A, the voltage range for the F031-06 sensor being limited to 25V, and the temperature range for the DHT 11 sensor ranging from -40°C to 125°C. Practical demonstrations were conducted using a 9V non-rechargeable alkaline battery, and the temperature sensor was tested under different environmental temperatures.

For the LoRa communication setup, the configuration and initialization process for both the sender and receiver nodes were elaborated upon. The following results were obtained by conducting practical demonstrations using a 9V non-rechargeable alkaline battery while varying the oil level. The circuit diagram and the sender node can be observed in Figure 4.9. In Figure 10, the receiver node displays temperature data and RSSI, with the receiver node being a Heltec ESP32 LoRa. In Figure 4.11, the results were shown on PuTTY, indicating a high oil level from counter 71 and RSSI 32. For further data analysis, PLX-DAQ, utilized in a previous study [8], was employed to evaluate the data in more depth.

Regarding the LoRa Sender configuration, it is essential to include the library that facilitates communication between the TTGO LoRa 32 and the LoRa transceiver module. Additionally, specific pins used by the LoRa Sender module must be specified. Within the `setup()` function, a manual software reset of the OLED using the RST pin is necessary. The LoRa transceiver module is then initialized by invoking the `begin()` method on the LoRa object, specifying the desired frequency as a parameter. Successful initialization is confirmed by a message displayed

on the OLED. In the `loop()` function, packet transmission occurs, initiated by the `beginPacket()` method. Data is incorporated into the packet using the `print()` method, and the packet is finalized using the `endPacket()` method.

For the LoRa Receiver setup, the syntax is similar to the sender setup, to streamline the LoRa configuration process, the appropriate library that facilitates seamless communication between the Heltec ESP32 and the LoRa transceiver module should be integrated. It is also crucial to explicitly define the pins used by the LoRa Receiver module. Within the `setup()` function, a manual software reset for the OLED is executed using the RST pin. This involves declaring the RST pin as an output, setting it to a LOW state, and then restoring it to a HIGH state. The user interface (U.I.) initialization concurrently initializes the display. To identify the LoRa receiver node, the designation "LORA RECEIVER" should be employed. In the `loop()` function, packets received are parsed using the `int packetSize = LoRa.parsePacket();` method to receive a packet from the sender module. The `while (LoRa.available()) {` loop is used to read the packet.

It is important to note that the results presented are from a lab test and do not represent data from an actual oil well pumping scenario. The LoRa Sender and Receiver setups require specific configuration and initialization steps to enable seamless communication between the modules. The LoRa system has been effectively utilized for data transmission and reception in this research, offering valuable insights into remote oil well monitoring. In summary, this study provides a comprehensive understanding of the environmental impact of abandoned wells and offers a practical solution through the implementation of solar-powered pumps and wireless monitoring using LoRa communication. The detailed insights and experimental setup will be valuable for addressing similar challenges in remote oil well monitoring and control. These results from this research will help facilitate oil well plugging but using renewable energy

sources and the cost of implementation and labour is cheaper than the cost of manual plugging per well.

## **5.2 Future Work**

In the scope of future work, the system modeling should be comprehensively performed using MATLAB, encompassing all the electrical devices' specifications. The model must accurately depict the electrical response under two distinct working conditions: when operating for 5 hours and when running non-stop. It is crucial to integrate the optimized system details from HOMERpro into the model to assess its compatibility with the intended operations. To facilitate system metering and data recording for historical analysis; a storage unit should be incorporated for data recording. This addition will automatically save real-time data, enabling valuable insights and references for future purposes.

## List of Publications

### ➤ *Articles in Refereed Publications*

•O. Chidolue and M. Tariq Iqbal, "Design and Performance Analysis of an Oil Pump Powered by Solar for a Remote Site in Nigeria," *European Journal of Electrical Engineering and Computer Science*, vol. 7, no. 1, pp. 62–69, Feb. 2023, doi: <https://doi.org/10.24018/ejece.2023.7.1.496>.

•O. Chidolue and T. Iqbal, "Real-time Monitoring and Data Acquisition using LoRa for a Remote Solar Powered Oil well " has been accepted for publication under the *International Journal of Applied Power Engineering (IJAPE)*

### ➤ *Refereed Conference Publications*

•O. Chidolue and T. Iqbal, "System Monitoring and Data logging using PLX-DAQ for Solar-Powered Oil Well Pumping," 2023 IEEE 13th Annual Computing and Communication Workshop and Conference (CCWC), Las Vegas, NV, USA, 2023, pp. 0690-0694, doi: 10.1109/CCWC57344.2023.10099099.

•S. U. Uddin, O. Chidolue, A. Azeez and T. Iqbal, "Design and Analysis of a Solar Powered Water Filtration System for a Community in Black Tickle-Domino," 2022 IEEE International IOT, Electronics and Mechatronics Conference (IEMTRONICS), Toronto, ON, Canada, 2022, pp. 1-6, doi: 10.1109/IEMTRONICS55184.2022.9795758.

### ➤ *Regional Conference Publications*

•O.Chidolue and M. Tariq Iqbal, "Design of a Solar Powered Pump for oil well in Nigeria presented at the 32nd Annual IEEE NECEC conference St. John's, 2022

# **APPENDICES**

## APPENDICES

### Appendix A

ARDUINO CODE EXPLANATION FOR PLX DAQ MONITORING SYSTEM AND RESULTS.

```
// CURRENT SENSOR SECTION AND PIN DEFINITION
```

```
int analogPin = A1; // Current sensor output
```

```
const int averageValue = 500; // This code reads the output value of the sensor 500 times and averages it.
```

```
long int sensorValue = 0; // variable to store the sensor value read
```

```
float voltage = 0;
```

```
float current = 0;
```

```
// FLOAT SWITCH SECTION AND PIN DEFINITION
```

```
int FloatSensor = 3;
```

```
int led = 8;
```

```
int buttonState = 1; //reads pushbutton status
```

```
void setup() {
```

```
    Serial.begin(9600);
```

```
    Serial.println("CLEARDATA");
```

```
    //define the column headings (PLX-DAQ command)
```

```
    Serial.println("LABEL,DATE,TIME, Oil level, current (A), voltage (V), Power (W), Temp (C)");  
    // setup serial
```

```
    pinMode(FloatSensor, INPUT_PULLUP);
```

```
    pinMode(led, OUTPUT);
```

```
}
```

```
void loop() {
```

```
    //FLOAT SWITCH UNIT
```

```

buttonState = digitalRead(FloatSensor);

if (buttonState == HIGH) {
    digitalWrite(led, HIGH);
} else {
    digitalWrite(led, LOW);
}

//CURRENT SENSOR UNIT

for (int i = 0; i < averageValue; i++)
{
    sensorValue += analogRead(analogPin);
// wait 2 milliseconds before the next loop
    delay(2);
}

sensorValue = sensorValue / averageValue;

voltage = sensorValue * 5.0 / 1024.0;

//When input is not connected and no load on output, the sensor has an initial voltage (Offset) of Vcc/2.

float current = (Voltage - 2.5) / 0.185; // CURRENT VALUE FROM SOURCE (PV PANEL), Offset value
is 2.5, sensitivity is 0.185

//Voltage Sensor Unit , the analog voltage resolution of the voltage sensor module is 5 V/1023 and from
the voltage divider unit in the sensor, the ratio between R1 and R2 is 5V

float VOLT = analogRead(A0)*5*5.0/1023; // VOLTAGE VALUE FROM POWER SOURCE(PV
PANEL)

float power = VOLT*current; // POWER CALCULATION

//TEMPERATURE SENSOR AND PIN DEFINITION

```

```

int tempRead = analogRead(A5);

float tempVolt = (float) tempRead / 1024.0 * 5; //multiply by 5V to get voltage

float tempCelsius = (tempVolt * 100.0) - 50.0; // converting to celsius by multiplying by 100 and
subtracting offset

Serial.print("DATA, DATE, TIME,"); // PLX-DAQ command

Serial.print(buttonState);

Serial.print(",");

Serial.print(current);

Serial.print(",");

Serial.print(VOLT);

Serial.print(",");

Serial.print(power);

Serial.print(",");

Serial.println(tempCelsius);

delay(1000);

}

```

The Arduino code below monitors the inverter's AC current measurement.

```

#include "ACS712.h"

ACS712 sensor(ACS712_05B, A1);

//ACS712_20A for 20 Amp type
//ACS712_30A for 30 Amp type

void setup()

Serial.begin(9600);

Serial.println("CLEARDATA");

//define the column headings (PLX-DAQ command)

```

```

Serial.println("LABEL,DATE,TIME, AC current (A)");
sensor.calibrate();
}
void loop() {
float I = sensor.getCurrentAC();
Serial.print("DATA, DATE, TIME,"); // PLX-DAQ command
Serial.println(I);
delay(300);
}

```

## APPENDIX B

### Lora Receiver

```

void loop() {
// try to parse packet
int packetSize = LoRa.parsePacket();
if (packetSize) {
// received a packets
Serial.print("Received packet. ");
display.clear();
display.setFont(ArialMT_Plain_16);
display.drawString(3, 0, "Received packet ");
display.display();
// read packet
while (LoRa.available()) {

```

```

currentTemperature = LoRa.readStringUntil('|');
Serial.print("Temp:");
Serial.println(currentTemperature);
currentVoltage = LoRa.readStringUntil('|');
Serial.print("Voltage (V):");
Serial.println(currentVoltage);
currentCurrent = LoRa.readStringUntil('|');
Serial.print("current(A):");
Serial.println(currentCurrent);
currentPower = LoRa.readStringUntil('|');
Serial.print("Power(W):");
Serial.println(currentPower);
currentButtonState = LoRa.readStringUntil('|');
Serial.print("OilLevel:");
Serial.println(currentButtonState);
currentCounter = LoRa.readStringUntil('|');
Serial.print("Counter:");
Serial.println(currentCounter);
}
// print RSSI of packet
Serial.print(" with RSSI ");
Serial.println(LoRa.packetRssi());
display.drawString(20, 45, "RSSI: ");

```

```
display.drawString(70, 45, (String)LoRa.packetRssi());  
  
display.display();
```

## APPENDIX C

### Lora Sender Code

```
#include <SPI.h>  
  
#include <LoRa.h>  
  
#include "SSD1306.h"  
  
#include <Arduino.h>  
  
#include <DHT.h>  
  
  
SSD1306 display(0x3c, 4, 15);  
  
#define SS 18  
  
#define RST 14  
  
#define DI0 26  
  
#define BAND 915E6 //Lora frequency for North America  
  
#define DHTTYPE DHT11  
  
#define DHT_PIN 13  
  
DHT dht(DHT_PIN, DHTTYPE);  
  
int sensor_reading = 0;  
  
float voltage = 0;  
  
int buttonState = 1; //reads pushbutton status for the oillevel  
  
int counter = 0  
  
void setup() {  
  
  pinMode(25,OUTPUT); //Send success, LED will bright 1 second  
  
  pinMode(16,OUTPUT);
```

```

digitalWrite(16, LOW); // set GPIO16 low to reset OLED
delay(50);
digitalWrite(16, HIGH);
dht.begin();
Serial.begin(115200);
while (!Serial);
display.init();
display.flipScreenVertically();
display.setFont(ArialMT_Plain_10);
display.setTextAlignment(TEXT_ALIGN_LEFT);
display.drawString(5,5,"LoRa Sender");
display.display();

SPI.begin(5,19,27,18);
LoRa.setPins(SS,RST,DIO);
Serial.println("LoRa Sender");
if (!LoRa.begin(BAND)) {
  Serial.println("Starting LoRa failed!");
  while (1);
}
Serial.println("LoRa Initial OK!");
display.drawString(5,20,"LoRa Initializing OK!");
display.display();
delay(2000);
}
void loop() {
  // Read temperature

```

```

float t = dht.readTemperature();

sensor_reading = analogRead(38);

voltage = sensor_reading *5* 3.3 / 4095;

float current=( analogRead(35)*(3.3/4095));

float power = voltage*current;

buttonState = digitalRead(15);

if (buttonState == HIGH) {
    digitalWrite(15, HIGH);
} else {
    digitalWrite(15, LOW);

}

Serial.print("Sending packet: ");

Serial.println(counter);

display.clear();

display.setFont(ArialMT_Plain_16);

display.drawString(3, 5, "Sending packet ");

display.drawString(50, 30, String(counter));

display.display();

// send packet

LoRa.beginPacket();

LoRa.print(t);

LoRa.print("|");

LoRa.print(voltage);

LoRa.print("|");

LoRa.print(current);

LoRa.print("|");

```

```

LoRa.print(power);

LoRa.print("|");

LoRa.print(buttonState);

LoRa.print("|");

LoRa.print(counter);

LoRa.endPacket();

counter++;

digitalWrite(25, HIGH); // turn the LED on (HIGH is the voltage level)

delay(1000);           // wait for a second

digitalWrite(25, LOW); // turn the LED off by making the voltage LOW

delay(1000);           // wait for a second

delay(3000);

}

```

## APPENDIX D

### Lora Receiver Code

```

#include <SPI.h>

#include <LoRa.h>

#include "SSD1306.h

SSD1306 display(0x3c, 4, 15);

#define SS    18

#define RST   14

#define DI0   26

#define BAND  915E6

String currentTemperature;

String currentVoltage;

String currentCurrent;

String currentPower;

```

```

String currentButtonState;

String currentCounter;

void setup() {

  pinMode(16,OUTPUT);

  digitalWrite(16, LOW); // set GPIO16 low to reset OLED

  delay(50);

  digitalWrite(16, HIGH);

  display.init();

  display.flipScreenVertically();

  display.setFont(ArialMT_Plain_10);

  display.setTextAlignment(TEXT_ALIGN_LEFT);

  Serial.begin(115200);

  while (!Serial); //if just the the basic function, must connect to a computer

  delay(1000);

  Serial.println("LoRa Receiver");

  display.drawString(5,5,"LoRa Receiver");

  display.display();

  SPI.begin(5,19,27,18);

  LoRa.setPins(SS,RST,DI0);

  if (!LoRa.begin(BAND)) {

    display.drawString(5,25,"Starting LoRa failed!");

    while (1);

  }

  Serial.println("LoRa Initial OK!");

  display.drawString(5,25,"LoRa Initializing OK!");

  display.display();

}

```

```

void loop() {
  // try to parse packet

  int packetSize = LoRa.parsePacket();

  if (packetSize) {
    // received a packets

    Serial.print("Received packet. ");

    display.clear();

    display.setFont(ArialMT_Plain_16);

    display.drawString(3, 0, "Received packet ");

    display.display();

    // read packet

    while (LoRa.available()) {
      currentTemperature = LoRa.readStringUntil('|');

      Serial.print("Temp:");

      Serial.println(currentTemperature);

      currentVoltage = LoRa.readStringUntil('|');

      Serial.print("Voltage (V):");

      Serial.println(currentVoltage);

      currentCurrent = LoRa.readStringUntil('|');

      Serial.print("current(A):");

      Serial.println(currentCurrent);

      currentPower = LoRa.readStringUntil('|');

      Serial.print("Power(W):");

      Serial.println(currentPower);

      currentButtonState = LoRa.readStringUntil('|');

      Serial.print("OilLevel:");

      Serial.println(currentButtonState);
    }
  }
}

```

```
currentCounter = LoRa.readStringUntil('|');  
  
Serial.print("Counter:");  
  
Serial.println(currentCounter);  
  
}  
  
// print RSSI of packet  
  
Serial.print(" with RSSI ");  
  
Serial.println(LoRa.packetRssi());  
  
display.drawString(20, 45, "RSSI: ");  
  
display.drawString(70, 45, (String)LoRa.packetRssi());  
  
display.display();  
  
}  
  
}
```